



**CHAOTIC VIBRATIONS OF THE
ONE-DIMENSIONAL WAVE EQUATION
DUE TO A SELF-EXCITATION
BOUNDARY CONDITION.
III. NATURAL HYSTERESIS
MEMORY EFFECTS**

GOONG CHEN*

*Department of Mathematics, Texas A&M University,
College Station, Texas 77843, USA*

SZE-BI HSU†

*Department of Mathematics, National Tsing Hua University,
Hsinchu 30043, Taiwan, R.O.C.*

JIANXIN ZHOU‡

*Department of Mathematics, Texas A&M University,
College Station, Texas 77843, USA*

Received May 18, 1997; Revised October 16, 1997

The nonlinear reflection curve due to a van der Pol type boundary condition at the right end becomes a multivalued relation when one of the parameters (α) exceeds the characteristic impedance value ($\alpha = 1$). From stability and continuity considerations, we prescribe kinematic admissibility and define hysteresis iterations with memory effects, whose dynamical behavior is herein investigated. Assume first that the left end boundary condition is fixed. We show that asymptotically there are two types of stable periodic solutions:

- (i) a single period- $2k$ orbit, or
- (ii) coexistence of a period- $2k$ and a period- $2(k + 1)$ orbits,

where as the parameter α increases, k will also increase and assume all positive integral values. Even though unstable periodic solutions do appear, there is obviously no chaos.

When the left end boundary condition is energy-injecting, however, we show that for a certain parameter range a shift sequence of subintervals of an invariant interval can be constructed and, therefore, chaos appears. Numerical simulations of chaotic and nonchaotic phenomena are also illustrated.

*E-mail: gchen@math.tamu.edu

†E-mail: sbhsu@am.nthu.edu.tw

‡E-mail: jzhou@math.tamu.edu

1. Introduction

In Part I [Chen *et al.*, 1998a], we have treated the one-dimensional wave equation

$$w_{tt}(x, t) - w_{xx}(x, t) = 0, \quad x \in (0, 1), \quad t > 0, \quad (1)$$

with fixed boundary condition at the left end:

$$w(0, t) = 0, \quad t > 0, \quad (2)$$

and a self-excitation boundary condition of van der Pol type at the right end:

$$w_x(1, t) = \alpha w_t(1, t) - \beta w_t^3(1, t), \quad t > 0; \quad \alpha, \beta > 0, \quad (3)$$

plus initial conditions

$$w(x, 0) = w_0(x), \quad w_t(x, 0) = w_1(x), \quad x \in (0, 1). \quad (4)$$

We have noted [Chen *et al.*, 1998a, Fig. 5] that if $\alpha > 1$ in (3), then the reflection relation F (cf. [Chen *et al.*, 1998a, (2.11)–(2.21)]) is multivalued, and thus the system (1)–(4) does not have the property of uniqueness of solutions. A single-valued branch of F with jump discontinuities was chosen in [Chen *et al.*, 1998b, (2.22)] through the action of some feedback control devices [Chen *et al.*, 1998a, Appendix C], which provides the uniqueness of solutions for (1)–(3). Such “uniqueness” is obtained through *artificial intervention*. However, we have learned from examples (see [Stoker, 1950, p. 95 and p. 137]) of vibrations in nonlinear mechanical and electronic systems that responses in such systems with hysteresis generally are *multivalued*. Among the several possible (and mathematically legitimate) multivalued branches, the physical nature of the system is such that the “most stable” branch and/or the “most continuous” route is preferred. These are the criteria we use to determine the kinematic admissibility of what we call natural *hysteresis iterates*. Therefore the perplexity of nonuniqueness is resolved. In this paper, we will study the dynamic response (1)–(4) for $\alpha > 1$ in (3) *in the sense that (3) corresponds to a natural hysteresis curve*.

The determination of a natural hysteresis loop corresponding to (3) is given in Sec. 2. The new reflection relation $u = F(v)$ now is defined through all three pieces (i.e. branches) of functions with partially overlapping domains but with a *directed*

path, containing a *memory effect*. The study of the dynamical behavior of iterates of maps defined through such natural hysteresis curves does not seem to have been done elsewhere before, to the best of our knowledge. Several examples of such hysteresis curves will be given.

In Sec. 3, we prove that for the natural hysteresis map corresponding to (3) with $\alpha > 1$, solutions of (1)–(4) are asymptotically either of a single even period (or, a single tone) or the mixing of exactly two successive even periods (i.e. a combination tone). The period grows with respect to α , but *there is no chaos*.

When energy is pumped in at the left end $x = 0$ as in Part II [Chen *et al.*, 1998b], the extra energy may cause instability and excite those (asymptotically) periodic vibrations (in Sec. 3) into chaotic vibrations. In Sec. 4, we show a sufficient condition for chaos to occur via the construction of a shift sequence.

Numerical simulations and graphics are also given in Secs. 3 and 4 to help visualize the dynamical behavior of solutions.

2. A Natural Hysteresis Map with Memory Effect

Inheriting the notations from Parts I and II [Chen *et al.*, 1998a, 1998b], for w in (1) we define the Riemann invariants

$$\begin{aligned} u(x, t) &= \frac{1}{2} [w_x(x, t) + w_t(x, t)], \\ v(x, t) &= \frac{1}{2} [w_x(x, t) - w_t(x, t)]. \end{aligned} \quad (5)$$

Then (u, v) satisfies a diagonalized first order hyperbolic system

$$\frac{\partial}{\partial t} \begin{bmatrix} u \\ v \end{bmatrix} = \begin{bmatrix} 1 & 0 \\ 0 & -1 \end{bmatrix} \frac{\partial}{\partial x} \begin{bmatrix} u \\ v \end{bmatrix}. \quad (6)$$

Example 2.1. Wave equation with fixed left end boundary condition and a self-excitation right end boundary condition. This problem is described by equations (1)–(4), with the additional constraint that $\alpha > 1$ in (3). It will be the focus of our attention in Sec. 3.

From (5), we convert the boundary condition (2) to the reflection relation

$$v = u. \quad (7)$$

Also, the boundary condition (3) now becomes the nonlinear reflection $u = F(v)$:

$$\beta(u - v)^3 + (1 - \alpha)(u - v) + 2v = 0, \tag{8}$$

at $x = 1$, any $t > 0$.

The curve $u = F(v)$ is multivalued when $\alpha > 1$ for $|v| \leq v^* \equiv [(\alpha - 1)/3] \sqrt{(\alpha - 1)/(3\beta)}$, cf. [Chen

et al., 1998a, Fig. 5] and Fig. 1. The overall shape of F is a “backward S ”.

The main objective of this section is to define the hysteresis iterates $u_{n+1} = F(u_n) = F^2(u_{n-1}) = \dots = F^{n+1}(u_0)$ which is physically natural for a multivalued relation F . Once the hysteresis iterates are well defined, the hyperbolic system (6)–(8) has a unique solution:

$$\left. \begin{aligned} &t = 2k + \tau, \quad k = 0, 1, 2, \dots, 0 \leq \tau < 2, \quad 0 \leq x \leq 1, \\ &v(x, t) = \begin{cases} F^k(v_0(x - \tau)), & \tau \leq x, \\ F^k(u_0(\tau - x)), & x < \tau \leq 1 + x, \\ F^{k+1}(v_0(2 - \tau + x)), & 1 + x < \tau \leq 2, \end{cases} \\ &u(x, t) = \begin{cases} F^k(u_0(x + \tau)), & \tau \leq 1 - x, \\ F^{k+1}(v_0(2 - x - \tau)), & 1 - x < \tau \leq 2 - x, \\ F^{k+1}(u_0(x + \tau - 2)), & 2 - x < \tau \leq 2, \end{cases} \end{aligned} \right\} \text{(cf. [Chen } et al., 1998a, (6.1), (6.2)] \tag{9}$$

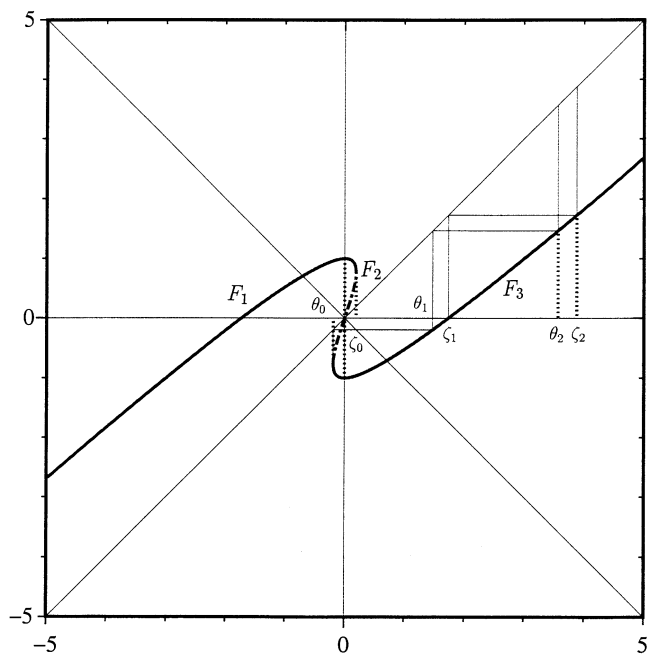


Fig. 1. The multivalued reflection relation $u = F(v)$ corresponding to (3) and (8), where $\alpha = 2, \beta = 1$ are used. This curve has a backward S shape, with three branches F_1, F_2 and F_3 . F_1 is defined on $(-\infty, v^*]$, F_2 on $[-v^*, v^*]$, and F_3 on $[-v^*, \infty)$. Here $\theta_0 = -v^*$. At $v = \hat{v}$, F_1 has a global maximum. (It happens in this case that $-\hat{v} = \zeta_0 = 0$.)

where

$$u_0(x) = \frac{1}{2} [w'_0(x) + w_1(x)],$$

$$v_0(x) = \frac{1}{2} [w'_0(x) - w_1(x)], \quad x \in [0, 1],$$

from (4) and (5).

The (u, v) -system in Example 2.1 is not alone in having a backward S -shaped curve. See the following for more examples.

Example 2.2. A self-excitation boundary condition with quadratic nonlinearity. Consider the vibrating system (1)–(4), but with (3) being replaced by

$$w_x(1, t) = \alpha w_t(1, t) - \beta |w_t(1, t)| w_t(1, t),$$

$$\alpha \geq 1, \beta > 0. \tag{10}$$

Then the rate of change of energy satisfies

$$\begin{aligned} \frac{d}{dt} E(t) &= \frac{d}{dt} \frac{1}{2} \int_0^1 [w_x^2(x, t) + w_t^2(x, t)] dx = \dots \\ &= \alpha w_t^2(1, t) - \beta |w_t(1, t)|^3 \\ &\times \begin{cases} \leq 0, & |w_t(1, t)| \geq \alpha/\beta, \\ & \text{if} \\ > 0, & |w_t(1, t)| < \alpha/\beta. \end{cases} \end{aligned} \tag{11}$$

Therefore the boundary condition (10) is also self-exciting (and self-regulating). The reflection relation $u = F(v)$ corresponding to (10) is determined from

$$\beta |u - v|(u - v) + (1 - \alpha)(u - v) + 2v = 0, \tag{12}$$

see Fig. 2 for an example. The derivative of this curve has a jump discontinuity at $(u, v) = (0, 0)$.

Example 2.3. Hysteresis curves as the composition of energy injecting and van der Pol boundary

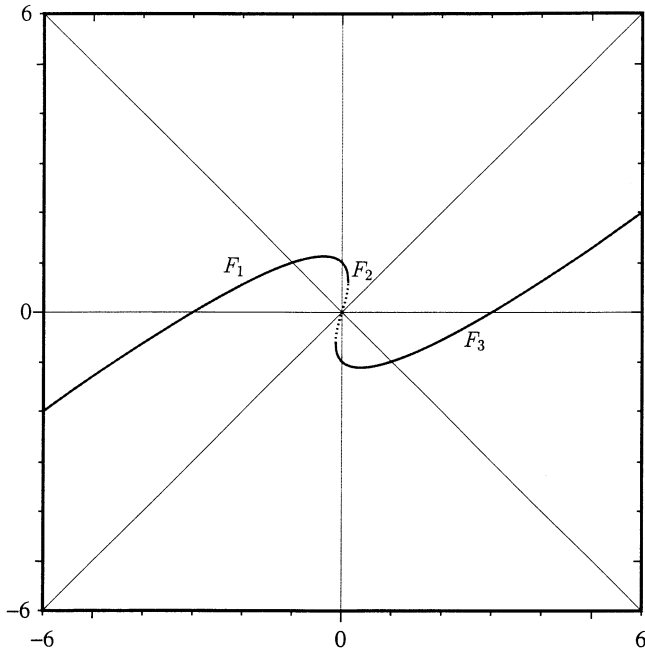


Fig. 2. The multivalued reflection relation $u = F(v)$ corresponding to (10) and (12), where $\alpha = 2, \beta = 1$ are used. Note that this curve also has a “backward S” shape similar to Fig. 1, with three branches F_1, F_2 and F_3 .

conditions. We now consider the system (1), (3) and (4), but with (2) changed to energy injection (Part II [Chen *et al.*, 1998b, (3)]):

$$w_t(0, t) = -\eta w_x(0, t), \quad 0 < \eta < 1. \quad (13)$$

Then as in [Chen *et al.*, 1998a, (1.8)–(1.12)], after converting the wave equation by (5) into a hyperbolic system for (u, v) , (13) yields the reflection relation

$$v = G(u) \equiv \frac{1 + \eta}{1 - \eta} u, \quad (0 < \eta < 1),$$

at $x = 0, \text{ for } t > 0. \quad (14)$

Let $u = F(v)$ be the same multivalued hysteresis curve as determined from (3):

$$\beta(u - v)^3 + (1 - \alpha)(u - v) + 2v = 0 \quad \text{at } x = 1,$$

for $t > 0, \quad \alpha > 1, \beta > 0,$

which forms the reflection condition at the right end. Then the solution formulas in Part II [Chen *et al.*, 1998b, (13), (14)] still *formally* applies:

For $t = 2k + \tau, k = 0, 1, 2, \dots, 0 \leq \tau < 2$, and for $0 \leq x \leq 1$,

$$u(x, t) = \begin{cases} (F \circ G)^k(u_0(x + \tau)), & \tau \leq 1 - x, \\ G^{-1} \circ (G \circ F)^{k+1}(v_0(2 - x - \tau)), & 1 - x < \tau \leq 2 - x, \\ (F \circ G)^{k+1}(u_0(\tau + x - 2)), & 2 - x < \tau \leq 2; \end{cases} \quad (15)$$

$$v(x, t) = \begin{cases} (G \circ F)^k(v_0(x - \tau)), & \tau \leq x, \\ G \circ (F \circ G)^k(u_0(\tau - x)), & x < \tau \leq 1 + x, \\ (G \circ F)^{k+1}(v_0(2 + x - \tau)), & 1 + x < \tau \leq 2. \end{cases} \quad (16)$$

In (15) and (16), the iterations of two multivalued relations are involved: $G \circ F$ and $F \circ G$. We have already seen the curve F in Part I [Chen *et al.*, 1998a, Fig. 5]. The shapes of $G \circ F$ and $F \circ G$ are illustrated in Figs. 3 and 4. The reader may find that the shapes of the curves corresponding to $G \circ F$ and $F \circ G$ again form a “backward S”. If we can make the “hysteresis iterates” of $G \circ F$ and $F \circ G$ well-defined in a physically natural way, then the formulas (15) and (16) will also become well defined.

This example will be our focus of attention in Sec. 4.

For our purposes, let us consider a general “multivalued backward S-shaped” relation $u = H(v) = H(\rho)(v)$, where ρ represents a parameter or

a set of parameters. Assume that H satisfies the following properties:

(i)
$$H = H_1 \cup H_2 \cup H_3; \quad (17)$$

- (ii) H_1 is a continuously differentiable function defined on $(-\infty, v^*]$ for some $v^* = v^*(\rho) > 0$, and H_3 is a function defined on $[-v^*, \infty)$ such that $H_1(v) = -H_3(-v)$, for all $v \in (-\infty, v^*]$;
- (iii) H_2 is an odd function defined on $[-v^*, v^*]$, continuously differentiable everywhere except perhaps at $v = 0$, such that $H_2'(v) > 1$ for all $[-v^*, v^*] \setminus \{0\}$;
- (iv) $H_1(v^*) = H_2(v^*)$;
- (v) $\lim_{v \rightarrow -\infty} H_1(v) = -\infty$;

(vi)

$$H_1(v) > H_2(v) > H_3(v), \quad H'_i(v) < H'_2(v), \quad (18)$$

$$i = 1, 3, \quad \text{for all } v \in (-v^*, v^*) \setminus \{0\};$$

(vii) There exists a unique $\hat{v} = \hat{v}(\rho) \in (-\infty, v^*)$, which is the (global) maximum of H_1 . Further, $H'_1(\hat{v}) = 0$,

$$H'_1(v) > 0 \quad \text{for all } v \in (-\infty, \hat{v}),$$

and

$$H'_1(v) < 0 \quad \text{for all } v \in (\hat{v}, v^*).$$

The reader may observe that all the curves displayed in Figs. 1–4 satisfy conditions (i)–(vii) above.

We are now in a position to give the following important definition.

Definition 2.1 (Hysteresis Iterates). Let H satisfy properties (i)–(vii) in (17)–(19). Let $u_0 \in \mathbb{R}$ and $k = 1, 2, 3, \dots$. We define the hysteresis iterates $u_k = H^k(u_0)$ by induction as follows:

(i) For $k = 1$, $u_1 \equiv H(u_0)$, where

$$u_1 = \begin{cases} H_1(u_0), & \text{if } u_0 < -v^*, \\ H_2(u_0), & \text{if } u_0 \in [-v^*, v^*], \\ H_3(u_0), & \text{if } u_0 > v^*. \end{cases} \quad (20)$$

(ii) For $k = 2$, $u_2 \equiv H^2(u_0)$, where

$$u_2 = \begin{cases} H_1(u_1), & \text{if either } u_1 \leq -v^* \text{ or if } u_0 < -v^* \text{ and } u_1 \in [-v^*, v^*], \\ H_2(u_1), & \text{if } u_0 \in [-v^*, v^*], u_1 \in (-v^*, v^*), \\ H_3(u_1), & \text{if either } u_1 \geq v^* \text{ or if } u_0 > v^* \text{ and } u_1 \in [-v^*, v^*], \end{cases} \quad (21)$$

for $u_1 = H(u_0)$.

(iii) Assume that $u_j = H^j(u_0)$ are defined for $j = 1, 2, \dots, k$, $k \geq 2$. We define $u_{k+1} = H^{k+1}(u_0)$ by

$$u_{k+1} = \begin{cases} H_1(u_k), & \text{if either } u_k \leq -v^* \text{ or if } u_{k-1} < -v^* \text{ and } u_k \in [-v^*, v^*], \\ H_2(u_k), & \text{if } u_0 \in [-v^*, v^*], u_1, u_2, \dots, u_k \in (-v^*, v^*), \\ H_3(u_k), & \text{if either } u_k \geq v^* \text{ or if } u_{k-1} > v^* \text{ and } u_k \in [-v^*, v^*]. \end{cases} \quad (22)$$

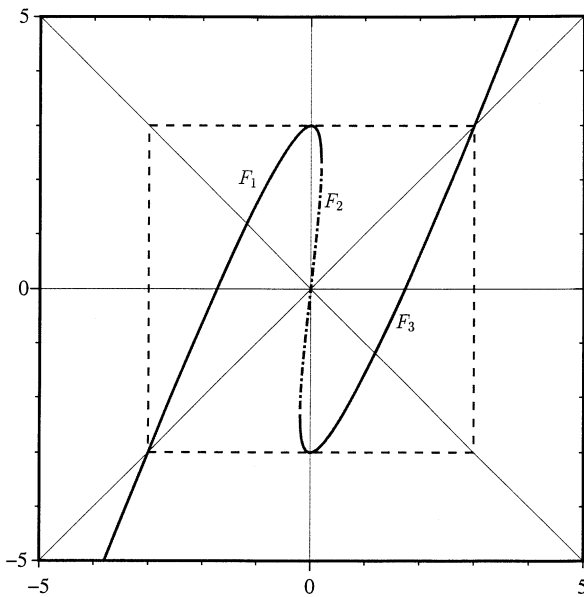


Fig. 3. The composite hysteresis curve $u = G \circ F(v)$ for Example 2.2, where $\eta = 1/2$, $\alpha = 2$, $\beta = 1$ are used. Note that the shape of the curve is a “backward S” with three branches F_1 , F_2 and F_3 .

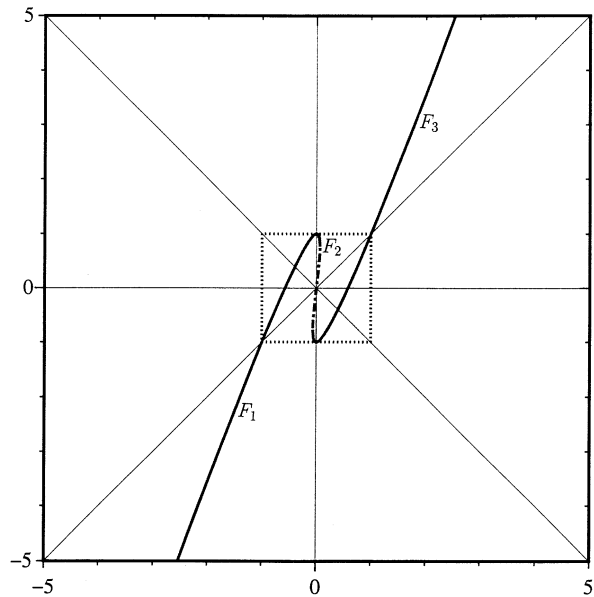


Fig. 4. The composite hysteresis curve $u = F \circ G(v)$ for Example 2.2, where $\eta = 1/2$, $\alpha = 2$, $\beta = 1$ are used. Note again that the shape of the curve is a “backward S” with three branches F_1 , F_2 and F_3 .

The above definition prescribes the *kinematic admissibility* regarding which branch should be chosen when multivaluedness comes into question, on the interval $[-v^*, v^*]$. It is based primarily on the following criteria:

- (i) stability: “nature” prefers stabler branches H_1 and H_3 over H_2 , cf. (18), except when the initial state starts from the neighborhood $[-v^*, v^*]$ of 0;
- (ii) continuity: “nature” also prefers continuity; when an iteration is performed along a certain branch H_i , it tends to continue along that same branch H_i until it has “run the entire course” of H_i .

We articulate these, among other things, in Remarks 2.1 and 2.2.

Remark 2.1. Intuitively, Definition 2.1 signifies the following facts:

- (i) In $(20)_2$, $(21)_2$ and $(22)_2$, we use the branch H_2 to perform iterations for $u_0 \in [-v^*, v^*]$, producing $u_1, u_2, \dots, u_j = H_2^j(u_0), \dots$, which is an *increasing* (resp. *decreasing*) *sequence* if $u_0 : 0 < u_0 < v^*$ (resp. $-v^* < u_0 < 0$); cf. (45) in Sec. 3. This iteration is stopped when $u_k > v^*$ (resp. $u_k < -v^*$). In that case, we switch iterations to the H_3 (resp. H_1) branch, as signified by $(21)_3$ and $(22)_3$ [resp. $(21)_1$ and $(22)_1$]. The H_2 branch is used only for $u_0 \in [-v^*, v^*]$. We may term this sequence of iterates $\{u_0, u_1, \dots, u_k\}$ the “maiden voyage” of u_0 . Once u_k falls outside $[-v^*, v^*]$, the H_2 branch will never be used any more because this branch is less stable than H_1 and H_3 due to the derivative condition in (18); H_1 and H_3 will then be used. Thus the maiden voyage is mostly a *transient response*.
- (ii) When we use the H_3 (resp. H_1) branch for iteration, we produce a *decreasing* (resp. *increasing*) *sequence* $u_j, u_{j+1}, u_{j+2}, \dots$; cf. (47) later. This sequence will eventually decrease (resp. increase) past $-v^*$ (resp. v^*). In that case, iteration by H_3 (resp. H_1) is no longer possible. We then switch to the H_1 (resp. H_3) branch. This is signified by $(21)_{1,3}$ and $(22)_{1,3}$.
- (iii) Definition 2.1 shows that the hysteresis iterates $H^k(u_0)$, $k = 1, 2, \dots$, have *memory effects*: $H^k(u_0)$ depends on *two preceding states* $H^{k-1}(u_0)$ and $H^{k-2}(u_0)$, if $k \geq 2$.

- (iv) Visintin [1986] (see also the references therein) has used set-valued functions to treat hysteresis. That approach is also applicable to our work, but the need to use it here is not really compelling. We choose instead to emphasize the physical motivations and connotations; see the next remark.

Remark 2.2. Definition 2.1 is obviously the most natural one from the physical point of view. To make this important point clear, let us present a plausible argument of kinematic admissibility as follows.

In a “gedanken experiment”, we may conceive a backward *S-shaped* curve H satisfying conditions (i)–(vii) in (17)–(19) as, say, a plot of stress versus strain (i.e. u versus v) of a one-dimensional nonlinear material, such as the material testing exemplar figure shown in [Parker et al., 1982, p. 452]. To determine the material response from the curve H , there are four possibilities involving the difficulty of multivaluedness of H for $v \in [-v^*, v^*]$:

- (i) v is originally zero and then begins to increase;
- (ii) v is originally zero and then begins to decrease (to negative values);
- (iii) $v > v^*$ originally and then begins to decrease;
- (iv) $v < -v^*$ originally and then begins to increase.

Other possibilities such as $v > v^*$ originally and then begins to increase are not worrisome, because in such a case the response will be moving along the H_3 branch rightward, without involving any multivaluedness of H .

Consider case (i). Experimentally (cf. [Parker et al., 1982, p. 452]), one finds that a sequence of increases of v from zero leads to a *sequence of corresponding increasing responses* u along the H_2 branch. This is the “maiden voyage” we referred to in Remark 2.1(i). But as v has increased past v^* , there will be a sudden downward jump of discontinuity of the response u , because it is no longer viable to move along the H_2 branch after $v > v^*$ (and the maiden voyage is over). Let v continue to increase. Then the response u will also increase, but along the H_3 branch, due to the fact that the previous downward jump discontinuity has brought the system to move along H_3 . This process and the input-output relation are illustrated in Fig. 5(a).

Case (ii) is similar to (i) by symmetry, so let us now look at case (iii). Let $v > v^*$ and consider a sequence of decreases of v . From the material’s natural, *continuity* property, this sequence of

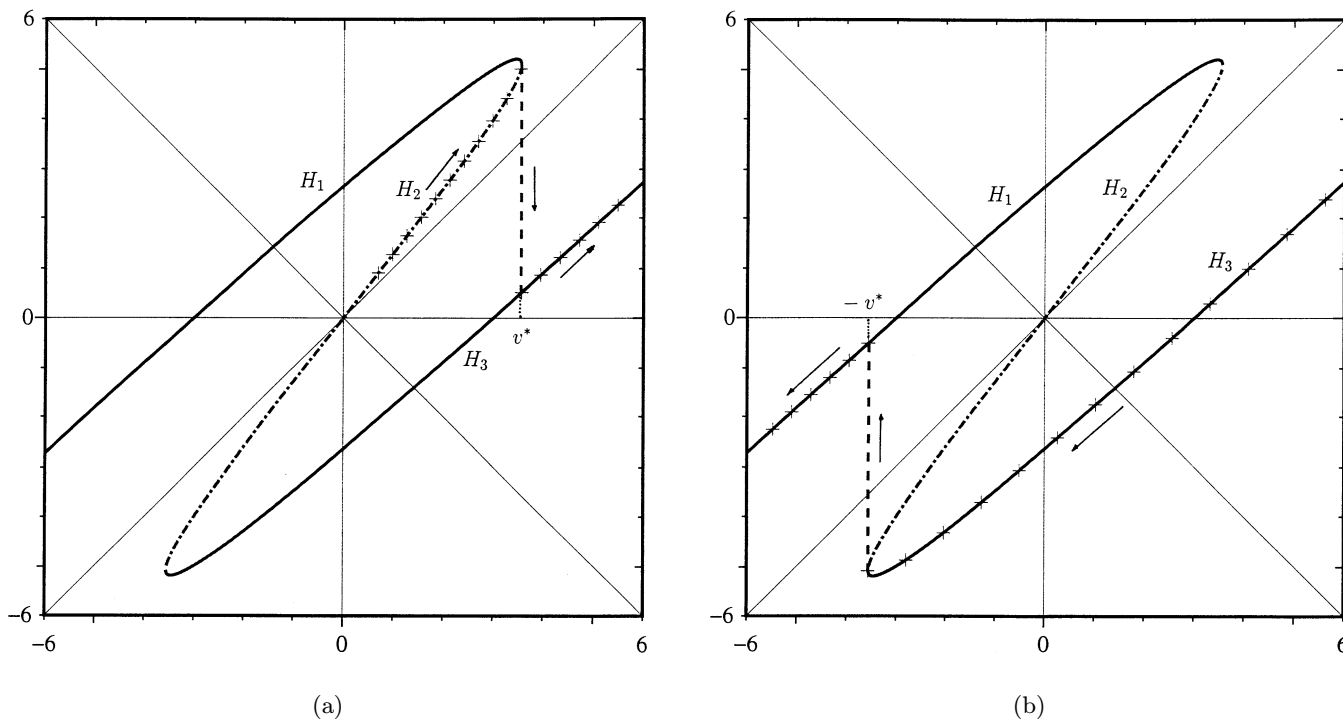


Fig. 5. (a) A “maiden voyage”: a sequence of increases of v near $v = 0$ leads to a corresponding sequence of increases of u along the H_2 branch, until $v = v^*$, where the system suffers a downward jump discontinuity. For v increasing past v^* , the system responses u will move rightward along the H_3 branch (and the maiden voyage is over in the sense that the system will never again respond according to the H_2 branch). (b) A nonmaiden voyage: let $v > v^*$ and let v decreases. Then the corresponding response u will move leftward along the H_3 branch, until $v = -v^*$, where the system cannot move any further leftward along H_3 and must take an upward jump discontinuity to the H_1 branch. It will then continue moving leftward along H_1 after v decreases past $-v^*$.

decreases of v will have the corresponding responses u on the H_3 branch, until v has decreased past $-v^*$, when it becomes no longer viable for the system to move any further leftward along the H_3 branch. The only admissible physical response is for the system to take an upward leap of jump discontinuity to the H_1 branch. This is exactly what is said in Remark 2.1(ii). For $v < -v^*$, the system response will move along the branch H_1 , for decreasing v . This process is illustrated in Fig. 5(b).

Case (iv) is similar to (iii) by symmetry.

Definition 2.1 is made possible because, as explained in Remarks 2.1 and 2.2, the iterates along any branch H_i , $i = 1, 2, 3$, form either a finite increasing or decreasing sequence; cf. (46), (47) and (49) later. The iterations then undergo an up or down jump discontinuity, and then the same behavior pattern is repeated. What if the iterates do not form an increasing or decreasing sequence as shown in the following Example 2.4? As of now, we do not know what is the most physically natural way to define the hysteresis iterates $u_k = H^k(u_0)$.

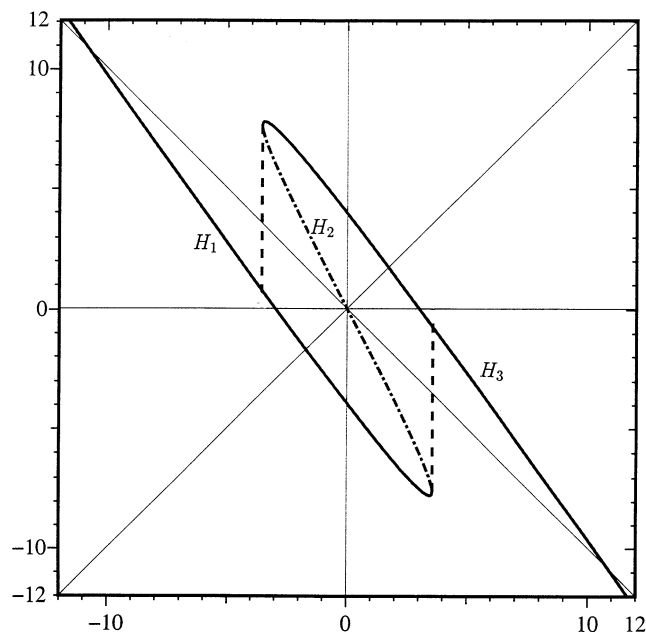


Fig. 6. A multivalued relation $u = H(v) = G \circ F(v)$ for Example 2.4, where $\eta = 8.0$, $\alpha = 2$, $\beta = 1$. Note that iterates along any branch H_1 , H_2 or H_3 will not yield an increasing or decreasing finite sequence, because two successive iterates have alternating signs.

Example 2.4. Consider the same model as in Example 2.3, but instead now let $\eta > 1$, similar to what we have done in Part II [Chen et al., 1998b]. Now the multivalued curve $u = G \circ F(v)$ is displayed as in Fig. 6. This curve has an *S* shape, but is *forward*, rather than backward. Since two successive iterates usually have alternating signs, we will not get any (locally) increasing or decreasing finite sequences.

We suspect that the hysteresis iterates $u_k = H^k(u_0)$ can still be defined by setting $u_k = (-1)^k(-H)^k(u_0)$, because $-H$ satisfies conditions (i)–(vii) in (17)–(19). But whether such a definition is physically natural or not remains debatable. We therefore will not treat the case of $\eta > 1$ in Sec. 4.

3. Cascades of Stable Periodic Solutions with Periods $2k$ and $2(k + 1)$

In this section, we consider (1)–(4). The only nonlinearity appears in the van der Pol type boundary condition (3) at $x = 1$. The boundary condition (2) at the left end $x = 0$ is linear and energy conserving. In this section, we show, by and large, that the only asymptotically stable solutions caused by the nonlinear hysteresis effects are either a *single tone* of period $2k$, or a *combination tone* of periods $2k$ and $2(k + 1)$. We conjecture that unstable solutions of period $2k$ also exist, but there is no chaos.

For clarity, let us summarize the equivalent hyperbolic system for (1)–(4) below:

$$\left\{ \begin{array}{l} \frac{\partial}{\partial t} \begin{bmatrix} u(x, t) \\ v(x, t) \end{bmatrix} = \begin{bmatrix} 1 & 0 \\ 0 & -1 \end{bmatrix} \frac{\partial}{\partial x} \begin{bmatrix} u(x, t) \\ v(x, t) \end{bmatrix}, \quad 0, x < 1, t > 0, \\ v(0, t) = u(0, t), \quad t > 0, \\ u(1, t) = F(v(1, t)), \quad t > 0; \quad F = F_{\alpha, \beta}, \alpha > 1, \beta > 0, \\ u(x, 0) = u_0(x) = \frac{1}{2} [w'_0(x) + w_1(x)], \quad v(x, 0) = v_0(x) = \frac{1}{2} [w'_0(x) - w_1(x)] \\ 0 < x < 1, \text{ cf. (4) and (5)}. \end{array} \right. \quad (23)$$

Note that in (23)₃, F has hysteresis and is defined as in Example 2.1. Let us reference Fig. 1 and its caption, and recall the following notation and facts:

$$x^* = x^*(\alpha, \beta) \equiv \sqrt{\frac{\alpha - 1}{3\beta}}, \quad (\text{cf. [Chen et al., 1998a, (2.15)]}) \quad (24)$$

$$v^* = v^*(\alpha, \beta) \equiv \frac{\alpha - 1}{3} \sqrt{\frac{\alpha - 1}{3\beta}} = \frac{\alpha - 1}{3} x^*, \quad (\text{cf. [Chen et al., 1998a, (2.16)]}) \quad (25)$$

$$\hat{v} = \hat{v}(\alpha, \beta) \equiv \frac{\alpha - 2}{3} \sqrt{\frac{\alpha + 1}{3\beta}}, \quad (26)$$

$$m = m(\alpha, \beta) \equiv \frac{\alpha + 1}{3} \sqrt{\frac{\alpha + 1}{3\beta}} = F_1(\hat{v}) = -F_3(-\hat{v}), \quad (F_1 \text{ takes a global maximum value } m \text{ at } \hat{v}) \quad (27)$$

$$F_1(v^*) = v^* + x^* = -F_3(-v^*), \quad (28)$$

$$F_3(v^*) = v^* - 2x^* = -F_1(-v^*), \quad (29)$$

$$-m < -(v^* + x^*) < -v^* < -\hat{v} < 0 < \hat{v} < v^* < v^* + x^* < m. \quad (30)$$

Define the iterates

$$\begin{aligned} \theta_0 = \theta_0(\alpha, \beta) = -v^* = -v^*(\alpha, \beta), \quad \zeta_0 = \zeta_0(\alpha, \beta) = -\hat{v} = -\hat{v}(\alpha, \beta) \\ F_3(\theta_{j+1}) = \theta_j, \quad F_3(\zeta_{j+1}) = \zeta_j, \quad j = 0, 1, 2, \dots, \end{aligned} \quad (31)$$

These iterates $\theta_i = \theta_i(\alpha, \beta)$, $\zeta_i = \zeta_i(\alpha, \beta)$, $i \in \mathbb{Z}^+$, and their *relative positions with respect to $\pm v^*$ and $\pm m$* , are *extremely important*. We will be relying on such information to determine the asymptotic behavior of the hysteresis iterates $u_{n+1} = F(u_n)$; see Theorems 3.1–3.8.

From the symmetry between F_1 and F_3 , we get

$$\begin{aligned} F_1(-\theta_{j+1}) &= -\theta_j, \\ F_1(-\zeta_{j+1}) &= -\zeta_j, \quad j = 0, 1, 2, \dots \end{aligned} \tag{32}$$

Lemma 3.1. *Let $\alpha > 1$ and $\beta > 0$. Let $F = F_1 \cup F_2 \cup F_3$ be the multivalued hysteresis relation as in Example 2.1 (and Fig. 1). Assume that $u = F_i(v)$, $i \in \{1, 2, 3\}$, for some $v \in \text{Dom}(F_i)$. Then*

$$u = v + cx^*, \tag{33}$$

where c is the unique solution of

$$(c + 2)(c - 1)^2 = -\frac{6}{\alpha - 1} \frac{v - v^*}{x^*}, \tag{34}$$

subject to the inequality constraint that

$$\left. \begin{aligned} c &\geq 1 \\ -1 &\leq c \leq 1 \\ c &\leq -1 \end{aligned} \right\} \text{ if } \begin{cases} i = 1, \\ i = 2, \\ i = 3. \end{cases} \tag{35}$$

Proof. The ideas are the same as those in Part I [Chen *et al.*, 1998a, Lemmas 3.1 and 3.2]. So we omit the details. ■

Lemma 3.2. *Let $\alpha > 1$ and $\beta > 0$. Then for the θ_j defined in (31), we have*

$$\theta_j = F_3(\theta_{j+1}) = \theta_{j+1} + c_{j+1}x^*, \quad j = 0, 1, 2, \dots, \tag{36}$$

where $c_j = c_j(\alpha)$, $i = 1, 2, 3, \dots$, depend only on α and are the unique solutions of

$$\begin{cases} c_j \leq -1, \\ (c_j + 2)(c_j - 1)^2 = \frac{6}{\alpha - 1} \sum_{i=1}^j c_i + 4. \end{cases} \tag{37}$$

Consequently,

$$\begin{aligned} \theta_j &= -\left(\sum_{i=1}^j c_i + \frac{\alpha - 1}{3}\right)x^*, \\ j &= 1, 2, \dots; \theta_1 < \theta_2 < \theta_3 < \dots \end{aligned} \tag{38}$$

Proof. The validity of (36) and (37) follows directly from (33), (34), (35)₃, (25) and (31)₁.

So let us now establish only (38). For $i = 1$, by (36), we have $\theta_0 = F_3(\theta_1) = \theta_1 + c_1x^* \Rightarrow \theta_1 = \theta_0 - c_1x^* = -(c_1 + \frac{\alpha-1}{3})x^*$ by (25) and (31)₁. Assume that (38) holds for i . Then for $i + 1$, by (36), we have

$$\begin{aligned} \theta_{i+1} &= \theta_i - c_{i+1}x^* = -\left(\sum_{j=1}^i c_j + \frac{\alpha - 1}{3}\right)x^* - c_{i+1}x^* \\ &= -\left(\sum_{j=1}^{i+1} c_j + \frac{\alpha - 1}{3}\right)x^*. \end{aligned}$$

So the induction process is complete. ■

Lemma 3.3. *Let $\alpha > 1$ and $\beta > 0$. Then for the ζ_j defined in (31) we have*

$$\zeta_j = F_3(\zeta_{j+1}) = \zeta_{j+1} + d_{j+1}x^*, \quad j = 0, 1, 2, \dots, \tag{39}$$

$$\begin{aligned} \zeta_j &= -\left(\sum_{k=0}^j d_k + \frac{\alpha + 1}{3} \sqrt{\frac{\alpha + 1}{\alpha - 1}}\right)x^*; \\ \zeta_0 &< \zeta_1 < \zeta_2 < \dots, \end{aligned} \tag{40}$$

where d_1, d_2, \dots , are the unique solutions of

$$\begin{cases} (d_j + 2)(d_j - 1)^2 - \frac{6}{\alpha - 1} \sum_{k=0}^j d_k \\ = 2\left(\frac{\alpha + 1}{\alpha - 1}\right)^{3/2} + 2, \quad j = 1, 2, \dots, \\ d_j \leq -1, \end{cases} \tag{41}$$

while

$$d_0 \equiv -\sqrt{\frac{\alpha + 1}{\alpha - 1}}. \tag{42}$$

Proof. First, note that if we define d_0 through

$$F_3(\zeta_0) = \zeta_0 + d_0x^* = -m,$$

then from (26), (27) and (31)₁ we get (42):

$$d_0 = -\frac{1}{x^*}(\zeta_0 + m) = -\sqrt{\frac{\alpha + 1}{\alpha - 1}}.$$

The rest, (41), can be established just as in the proof of Lemma 3.2. ■

We collect a bunch of numerical facts together to form the following potpourri lemma.

Lemma 3.4. *Let $\alpha > 1$ and $\beta > 0$. Then*

- (i) $m < \theta_1$ if and only if $1 < \alpha < 2.6994$, and $m = \theta_1$ if $\alpha = 2.6994$;
- (ii) $F_1(v^*) = v^* + x^* < \theta_1$ if and only if $1 < \alpha < 2.9131$, and $v^* + x^* = \theta_1$ if $\alpha = 2.9131$;
- (iii) $\zeta_1 < m$ if and only if $1 < \alpha < 2.9664$, and $\zeta_1 = m$ if $\alpha = 2.9664$;
- (iv) $F_3(v^*) = v^* - 2x^* \geq -v^*$ if and only if $\alpha \geq 4$;
- (v) $F_3(v^*) = v^* - 2x^* \geq -\theta_1$ if and only if $1 < \alpha \leq 4$;
- (vi) $\theta_1 \geq v^*$ if and only if $1 < \alpha \leq 4$;
- (vii) $m < \theta_2$ if and only if $1 < \alpha < 5.2935$;
- (viii) $F_3'(v) < 0$ for $v \in (-v^*, -\hat{v})$, $F_3'(-\hat{v}) = 0$, and $0 < F_3'(v) < 1$ for $v \in (-\hat{v}, \infty)$.
Similarly,

$$F_1'(v) < 0 \text{ for } v \in (\hat{v}, v^*), F_1'(\hat{v}) = 0,$$

$$\text{and } 0 < F_1'(v) < 1 \text{ for } v \in (-\infty, \hat{v}). \quad (43)$$

Proof. The values of α satisfying the inequalities can be easily computed by applying Lemmas 3.2 and 3.3. We omit the details. ■

For $v \in (v^*, \infty)$, F is single-valued and $F(v) = F_3(v)$. Now consider the iterates $F_3^n(v_0)$ for some $v_0 \in (v^*, \infty)$. Then according to the definition of hysteresis iterates (20)–(22) by letting $H = F$ therein, we get

$$F_3^j(v_0) = F^j(v_0), \quad \text{if } F_3^j(v_0) \in [-v^*, \infty),$$

$$j = 1, 2, \dots$$

The above remains valid even for $j = n$, where $F_3^n(v_0) \notin [-v^*, \infty]$ but $F_3^{n-1}(v_0) \in [-v^*, \infty)$. But for $j > n$, it is no longer possible to form the iterates $F_3^j(v_0)$. By the definition of hysteresis iterates, we leap up and iterate along the F_1 branch, and get

$$F_1 \circ F_3^n(v_0) = F^{n+1}(v_0). \quad (44)$$

This simple observation also shows that in general $F_1 \circ F_3^k(v_0) \neq F^{k+1}(v_0)$ even though $F_3^k(v_0) \in \text{Dom}(F_1)$, because $F_3^k(v_0)$ “has not run the entire course along the branch F_3 ”. The following simple proposition is useful in deciding whether (44) holds.

Proposition 3.1. *Let $\alpha > 1, \beta > 0$ and $v_0 \in \mathbb{R}$.*

- (i) *If $v_0 \in (0, v^*)$ such that $F_2(v_0), F_2^2(v_0), \dots, F_2^j(v_0) \in (0, v^*]$, then*

$$0 < F_2(v_0) < F_2^2(v_0) < \dots < F_2^j(v_0). \quad (45)$$

Similarly, if $v_0 \in (-v^, 0)$ such that $F_2(v_0), F_2^2(v_0), \dots, F_2^j(v_0) \in [-v^*, 0)$, then*

$$0 > F_2(v_0) > F_2^2(v_0) > \dots > F_2^j(v_0). \quad (46)$$

- (ii) *Let $i \geq 1$ such that $F^{i-1}(v_0), F^i(v_0) \in (v^*, \infty)$. If for $w = F^i(v_0)$, we have $F_3(w), F_3^2(w), \dots, F_3^j(w) \in [-v^*, \infty)$, then*

$$F_3(w) > F_3^2(w) > \dots > F_3^j(w) \geq -v^*,$$

$$F_3^j(w) = F_3^j(F^i(v_0)) = F^{i+j}(v_0). \quad (47)$$

Furthermore, if $F_3^{n-1}(w) \in [-v^, \theta_1)$, then*

$$F^{n+1}(w) = F_1 \circ F_3^n(w) = F^{n+1+i}(v_0). \quad (48)$$

Conversely, if $F^{n-1}(w) \notin [-v^, \theta_1)$, then (48) does not hold.*

- (iii) *Let $i \geq 1$ such that $F^{i-1}(v_0), F^i(v_0) \in (-\infty, -v^*)$. If for $w = F^i(v_0)$, we have $F_1(w), F_1^2(w), \dots, F_1^j(w) \in (-\infty, v^*]$, then*

$$F_1(w) < F_1^2(w) < \dots < F_1^j(w) \leq v^*,$$

$$F_1^j(w) = F_1^j(F^i(v_0)) = F^{i+j}(v_0). \quad (49)$$

Furthermore, if $F_1^{n-1}(w) \in (-\theta_1, v^]$, then*

$$F^{n+1}(w) = F_3 \circ F_1^n(w) = F^{n+1+i}(v_0). \quad (50)$$

Conversely, if $F_1^{n-1}(w) \notin (-\theta_1, v^]$, then (50) does not hold.*

Proof. Because F_2 is odd, strictly increasing on $[-v^*, v^*]$ and lying above the diagonal line $u = v$ on $[0, v^*]$, we easily get (45) and (46).

Now, consider (ii). The memory effect that $F^{i-1}(v_0), F^i(v_0) \in (v^*, \infty)$ implies that for $w = F^i(v_0)$, the iterates $F(w), F^2(w), \dots$, are obtained by iterations along the F_3 branch. The F_3 branch lies below the diagonal line $u = v$, is strictly increasing on $(-\hat{v}, \infty]$ but strictly decreasing on $[-v^*, -\hat{v})$. Using Lemma 3.1 and the same ideas as in the proof of (38) in Lemma 3.2, we can easily show the monotonicity of (47). Details are omitted.

To show (48), first we note that since $F_3^{n-1}(w) \in [-v^*, \theta_1]$, we can still make a final iteration along the F_3 branch and get

$$F_3^n(v_0) = F_3(F_3^{n-1}(w)) = F^n(w)$$

$$= F^n(F^i(v_0)) = F^{n+i}(v_0).$$

Using the fact from (31) and Lemma 3.4 that

$$\begin{aligned} F_3([-v^*, -\hat{v}] \cup [-\hat{v}, \theta_1]) &= F_3([-v^*, -\hat{v}]) \cup F_3([-\hat{v}, \theta_1]) \\ &= [-m, -(v^* + x^*)] \cup [-m, -v^*] = [-m, -v^*], \end{aligned}$$

we get $F^n(w) = F_3(F^{n-1}(w)) \in [-m, -v^*]$, and therefore

$$\begin{aligned} F^{n+1}(w) &= F(F^n(w)) = F_1(F^n(w)) = F_1 \circ (F_3^n(F^i(v_0))) \\ &= F^{n+1}(F^i(v_0)) = F^{n+1+i}(v_0), \end{aligned}$$

and (48) is proved.

The converse part can be argued the same way. We omit the details. Part (iii) follows from part (ii) by symmetry. ■

3.1. Asymptotically stable solutions of periods two and four for α close to 1

Theorem 3.1. *Let $\alpha : 1 < \alpha \leq 2.6694$ so that $v^* < m \leq \theta_1$. Then there exists a unique period-2 point $\xi : \xi = F^2(\xi)$, $\xi \in [v^*, m]$, which is a global attractor.*

Proof. Since $v^* < m \leq \theta_1$ and F_3 is strictly monotonically increasing on $[v^*, \theta_1]$, we have

$$-m = \min_{v \geq -v^*} F_3(v) < F_3(v^*) < F_3(m) \leq F_3(\theta_1) = -v^*.$$

Therefore

$$F_3([v^*, m]) = [F_3(v^*), F_3(m)] \subseteq [-m, -v^*].$$

By symmetry,

$$F_1([-m, -v^*]) = [F_1(-m), F_1(-v^*)] \subseteq [v^*, m].$$

Hence by Proposition 3.1(ii), we have

$$F^2 = F \circ F = F_1 \circ F_3 : [v^*, m] \rightarrow [v^*, m].$$

Therefore, by using the Intermediate Value Theorem, we obtain a point $\xi \in [v^*, m]$ such that $F^2(\xi) = \xi$. This ξ is unique and attracting because by Lemma 3.4(viii) we have some $c : 0 < c < 1$ such that

$$0 < F_3'(v) < c < 1, \quad \text{for } v \in [v^*, m]; \quad 0 < F_1'(v) < c < 1, \quad \text{for } v \in [-m, -v^*].$$

Now it remains to show that the iterates of any point v will eventually enter $[v^*, m]$. Since the interval $[-m, m]$ is a global attractor for the hysteresis iterates $v_{n+1} = F(v_n)$, cf. Part II [Chen *et al.*, 1998b, Lemma 2.5], we need only show that points in $[-v^*, v^*]$ are attracted to $[-m, -v^*]$ by the action of F_3 , and that points in $[-v^*, v^*]$ are attracted to $[v^*, m]$ by the action of F_1 . This is easy:

$$F_3([-v^*, v^*]) \subseteq [-m, F_3(v^*)] = [-m, v^* - 2x^*] \subseteq [-m, -v^*] \quad [\text{cf. (29) and Lemma 3.4(iv)}].$$

A similar statement holds for F_1 .

The proof is complete. ■

Next, we increase α and consider the situation $v^* + x^* < \theta_1 < m$. By Lemma 3.4, this holds if and only if $2.6994 < \alpha < 2.9131$. This situation turns out to be a little complicated.

Theorem 3.2. *Let $\alpha : 2.6994 < \alpha < 2.9131$ so that $v^* + x^* < \theta_1 < m$. Then*

- (i) *there exists a unique period-2 point $\xi \in (v^*, \theta_1)$ such that $F^2(\xi) = \xi$;*
- (ii) *if, in addition, $\alpha < \alpha^* = 2.8284$, then the period-2 orbit in (i) is globally attracting;*
- (iii) *if $\alpha > \alpha^*$, then there exist an unstable period-4 orbit as well as another period-4 orbit.*

Proof.

- (1) We first show the existence of a period-2 orbit. Since $F_3(\theta_1) = -v^*$, and

$$F_3(v^*) = v^* - 2x^* \quad [\text{by (29)}]$$

$$> -\theta_1 \quad [\text{by Lemma 3.4(v)}], \quad (51)$$

we have

$$F_3 : [v^*, \theta_1] \xrightarrow{\text{into}} [-\theta_1, -v^*].$$

Similarly, $F_1 : [-\theta_1, -v^*] \xrightarrow{\text{into}} [v^*, \theta_1]$. From the strict contraction property in (43), we see that $F_1 \circ F_3 : [v^*, \theta_1] \rightarrow [v^*, \theta_1]$ is a strict contraction. Therefore, there exists a unique period-2 point $\xi \in (v^*, \theta_1)$ such that $F^2(\xi) = \xi$.

- (2) Let us determine the domain of attraction of the period-2 orbit of ξ . Since $v^* + x^* < \theta_1$ and $F_3(v^*) > -\theta_1 > -m$ by the assumption and (51), there exist $\delta_1, \delta_2 : -v^* < \delta_2 < \delta_1 < v^*$ such that $F_3(\delta_2) = F_3(\delta_1) = -\theta_1$. Therefore

$$[-v^*, \delta_2) \cup (\delta_1, \theta_1] \subseteq W^s(\xi),$$

the stable set of ξ , (52)

$$F_3 : [\delta_2, \delta_1] \rightarrow [-m, -\theta_1],$$

$$F_1 : [-m, -\theta_1] \rightarrow [F_1(-m), v^*]. \quad (53)$$

There are two possibilities:

- (a) If $F_1(-m) > -\delta_2$, then $F_1([-m, -\theta_1]) \subseteq [-\delta_2, v^*]$ from (53), and $F_1 \circ F_1([-m, -\theta_1]) \subseteq F_1([-m, -\theta_1]) \subseteq [v^* + x^*, \theta_1]$. Thus $[\delta_2, \delta_1] \subseteq W^s(\xi)$.
 Since $F_1(-m) > -\delta_2$ if and only if $F_3(m) < \delta_2$, we also have $[\theta_1, m] \subseteq W^s(\xi)$. We conclude that the period-2 orbit of ξ is globally attracting.
- (b) If $F_1(-m) \leq -\delta_2$, equivalently, $F_3(m) \geq \delta_2$, then there exists $\gamma_1 : \theta_1 < \gamma_1 \leq m$ such that $F_3(\gamma_1) = \delta_2$. It follows that $F_3([\theta_1, \gamma_1]) =$

$[-v^*, \delta_2]$, and by (52), we have $[\theta_1, \gamma_1] \subseteq W^s(\xi)$.

For case (b) above, since we have $F_3(\gamma_1) = \delta_2$ as well as $F_1(-\gamma_1) = -\delta_2$, we can find δ_3 and δ_4 such that

$$-v^* < \delta_2 < \delta_4 < \delta_3 < \delta_1 < v^*,$$

$$F_3(\delta_4) = F_3(\delta_3) = -\gamma_1.$$

Then we obtain $F_3([\delta_4, \delta_3]) \subseteq (-m, -\gamma_1)$. Again, two possible cases occur:

- (c) If $F_1(-m) > -\delta_4$, then

$$F_1 \circ F_1((-m, -\gamma_1)) \subseteq F_1(-\delta_4, -\delta_2) = (\theta_1, \gamma_1),$$

and thus $(\delta_4, \delta_3) \cup (-m, -\gamma_1) \subseteq W^s(\xi)$, and hence the period-2 orbit of ξ is a global attractor.

- (d) If $F_1(-m) \leq -\delta_4$, equivalently, $F_3(m) \geq \delta_4$, then there exists $\gamma_2 : \theta_1 < \gamma_1 < \gamma_2 \leq m$ such that $F_3(\gamma_2) = \delta_4$. We can further find δ_5 and δ_6 such that

$$-v^* < \delta_2 < \delta_4 < \delta_6 < \delta_5 < \delta_3 < \delta_1 < v^*,$$

$$F_3(\delta_5) = F_3(\delta_6) = -\gamma_2.$$

According to the discussions in (a)–(d) above, we can continue the process to construct $\delta_1, \delta_2, \dots, \delta_{2n-1}, \delta_{2n}; \gamma_1, \gamma_2, \dots, \gamma_n$. If $F_3(m) < \delta_{2n}$ for some $n \in \mathbb{Z}^+$, we stop and conclude that the period-2 orbit of ξ is a global attractor. Otherwise, $F_3(m) > \delta_{2n}$ holds for all $n \in \mathbb{Z}^+$ and we have sequences $\{\gamma_n\}, \{\delta_{2n}\}, \{\delta_{2n+1}\}$ such that

$$\gamma_1 < \gamma_2 < \dots < \gamma_n < \dots \uparrow \tilde{\gamma},$$

$$\delta_1 > \delta_3 > \dots > \delta_{2n+1} > \dots \downarrow \delta_R,$$

$$\delta_2 < \delta_4 < \dots < \delta_{2n} < \dots \uparrow \delta_L.$$

for some $\tilde{\gamma}, \delta_R, \delta_L \in \mathbb{R}$ as the unique limits of these bounded monotonic sequences. By the same reasoning as in (a)–(d), we conclude that

$$(-v^*, \delta_L) \cup (\delta_R, v^*) \subseteq W^s(\xi),$$

$$F_3(\tilde{\gamma}) = \delta_L, \quad F_3(\delta_L) = -\tilde{\gamma},$$

$$F_1(-\tilde{\gamma}) = -\delta_L, \quad F_1(-\delta_L) = \tilde{\gamma}.$$

The above gives $F_1^2 \circ F_3^2(\tilde{\gamma}) = F^4(\tilde{\gamma}) = \tilde{\gamma}$, and thus $\{\tilde{\gamma}, \delta_L, -\tilde{\gamma}, -\delta_L\}$ forms a period-4 orbit. This orbit is obviously unstable.

In addition, we also have

$$F_3^2([\tilde{\gamma}, m]) \subseteq F_3([\delta_L, \delta_R]) \subseteq [-m, -\tilde{\gamma}],$$

$$F_1^2([-m, -\tilde{\gamma}]) \subseteq F_1([-m, -\delta_L]) \subseteq [\tilde{\gamma}, m].$$

Therefore $F^4([\tilde{\gamma}, m]) \subseteq [\tilde{\gamma}, m]$, and a period-4 orbit exists which is distinct from the previous unstable period-4 orbit.

Denote

$$\alpha^* \equiv \inf\{\alpha \in (2.6994, 2.9131)\}$$

$$F_3(m) = F_3(m(\alpha)) > \delta_{2n}, \quad \forall n = 1, 2, \dots\}.$$

Then at least two period-4 orbits exist if $\alpha > \alpha^*$. If $\alpha < \alpha^*$, then the period-2 orbit of ξ is globally attracting.

Through direct computations, we have found

$$\alpha^* \approx 2.8284 \quad \blacksquare$$

Remark 3.1. More elaborate analysis [Chern, 1995, Lemma 4.7] shows that besides the unstable period-4 orbit in Theorem 3.2(iii), the second period-4 orbit is unique and attracting. Furthermore, $\alpha = \alpha^*$ is a value where *saddle-node (tangent) bifurcation* occurs.

In Theorem 3.2, the condition $v^* + x^* < \theta_1$ is required. What happens if $\theta_1 \leq v^* + x^*$, i.e. $\alpha \geq 2.9131$? This is answered in the following by increasing α past 2.9131.

Theorem 3.3. *Let $\theta_1 \leq v^* + x^*$ and $\zeta_1 < m$, equivalently, $2,9131 \leq \alpha < 2.9664$. Then there exists a unique period-2 point $\xi_1 \in [v^*, \theta_1)$ whose period-2 orbit is globally attracting on $[v^*, \theta_1)$, and a unique period-4 point $\xi_2 \in [\zeta_1, m]$ whose period-4 orbit is globally attracting on $[\zeta_1, m]$.*

Proof. Since $2.9131 \leq \alpha < 2.9664$, by Lemma 3.4, we have

$$v^* < \theta_1 < m < \theta_2 \quad \text{and} \quad v^* < \theta_1 < \zeta_1 < m.$$

Also

$$F_3(v^*) = v^* - 2x^* > -\theta_1, \quad \text{by Lemma 3.4(v)}.$$

Therefore

$$F_3 : [v^*, \theta_1] \xrightarrow{\text{onto}} [v^* - 2x^*, -v^*] \subseteq [-\theta_1, -v^*].$$

Similarly,

$$F_1 : [-\theta_1, -v^*] \longrightarrow [v^*, \theta_1].$$

By (43), $F^2 = F_1 \circ F_3 : [v^*, \theta_1] \rightarrow [v^*, \theta_1]$ is a strict contraction. Therefore F^2 has a unique fixed point $\xi_1 \in [v^*, \theta_1)$ with domain of attraction containing $[v^*, \theta_1)$. This point ξ_1 has period-2.

Next, consider

$$\begin{aligned} [\zeta_1, m] &\xrightarrow{F_3} [F_3(\zeta_1), F_3(m)] \\ &= [-\hat{v}, F_3(m)] \xrightarrow{F_3} [F_3(-\hat{v}), F_3^2(m)] \\ &= [-m, F_3^2(m)] \subseteq [-m, -\zeta_1], \end{aligned}$$

where we have used the strict contraction property (43) of F_3 to get $F_3^2(m) \leq -\zeta_1 < -v^*$. Therefore $F_3^2 : [\zeta_1, m] \rightarrow [-m, -\zeta_1]$. Similarly, $F_1^2 : [-m, -\zeta_1] \rightarrow [\zeta_1, m]$. Hence

$$F^4 = F_1^2 \circ F_3^2 : [\zeta_1, m] \rightarrow [\zeta_1, m]$$

is a strict contraction by Lemma 3.4(viii). Therefore, there exists a unique fixed point $\xi_2 \in [\zeta_1, m]$ with domain of attraction containing $[\zeta_1, m]$. This point ξ_2 has period-4. \blacksquare

Further increasing α , we obtain the following.

Theorem 3.4. *Let $v^* < \theta_1 < m < \theta_2$, $m < \zeta_1$, $-m < F_3(-v^*) = -(v^* + x^*) < -\theta_1$, equivalently, $2.9664 < \alpha < 4$. Then there exists a period-4 point $\xi \in [v^* + x^*, m]$.*

Proof. We have

$$\begin{aligned} [\theta_1, \zeta_1] &\xrightarrow{F_3} [-v^*, -\hat{v}] \xrightarrow{F_3} [-m, F_3(-v^*)] \\ &\subseteq [-m, -(v^* + x^*)] \subseteq [-m, -\theta_1], \end{aligned}$$

Similarly,

$$\begin{aligned} [-\zeta_1, -\theta_1] &\xrightarrow{F_1} [\hat{v}, v^*] \xrightarrow{F_1} [F_1(v^*), m] \\ &= [v^* + x^*, m] \subseteq [\theta_1, m]. \end{aligned}$$

Therefore by Proposition 3.1, $F^4 = F_1^2 \circ F_3^2 : [v^* + x^*, m] \rightarrow [v^* + x^*, m]$, and there exists a fixed point $\xi \in [v^* + x^*, m]$. It is a period-4 point. \blacksquare

Theorem 3.5. *Let $\theta_1 \leq v^*$ and $m < \theta_2$, equivalently, $4 \leq \alpha < 5.2935$. Then there exists a unique period-4 orbit, and no other periods exist. Furthermore, let $\psi \in (-v^*, -\hat{v})$ satisfy $F_3'(\psi) = -1$. If $F(v^*) > \psi$ is satisfied, then the period-4 orbit is unique and globally attracting.*

Proof. By Lemma 3.4(v)–(vii), we have

$$\begin{aligned} \theta_1 &\leq v^* < m < \theta_2 \\ \text{and} \quad -v^* &\leq F_3(v^*) = v^* - 2x^* < -\theta_1. \end{aligned}$$

Then $v^* < m < \theta_2$ implies $F_3(m) < F_3(\theta_2) = \theta_1$, and

$$[v^*, m] \xrightarrow{F_3} [F_3(v^*), F_3(m)] \subseteq [-v^*, \theta_1],$$

$$[F_3(v^*), F_3(m)] \xrightarrow{F_3} [F_3^2(v^*), F_3^2(m)] \subseteq [-m, -v^*].$$

Similarly,

$$[-m, -v^*] \xrightarrow{F_1} [F_1(-m), F_1(-v^*)] \subseteq (-\theta_1, v^*],$$

$$[F_1(-m), F_1(-v^*)] \xrightarrow{F_1} [F_1^2(-m), F_1^2(-v^*)] \subseteq (v^*, m].$$

Hence by Proposition 3.1, $F^4 = F_1^2 \circ F_3^2 : [v^*, m] \rightarrow [v^*, m]$. Using the Intermediate Value Theorem, we see that F^4 has a fixed point, which in turn is a prime period-4 point of F . From the itinerant intervals of $F^4 = F_1 \circ F_1 \circ F_3 \circ F_3$ as shown above, one can show that the intersection of $u = F^4(v)$ and $u = v$ on $[v^*, m] \times [v^*, m]$ can happen at most at four points. Each point has period-4, and hence intersection happens at exactly four points. There exists a unique period-4 point $\xi \in [v^*, m]$.

Making a slightly more detailed argument, one can show that all points on $[-m, m]$ are eventually mapped into $[v^*, m] \cup [-v^*, \theta_1]$. Therefore, no other periods exist but period-4.

Since $F_3'(-v^*+) = -\infty$ and $F_3'(-\hat{v}) = 0$, there exists a point $\psi \in (-v^*, -\hat{v})$ such that $F_3'(\psi) = -1$. If $F_3(v^*) > \psi$, then since $0 < F_3'(v) < 1$ on $[v^*, m]$ and $|F'(v)| < 1$ on $[F_3(v^*), F_3(m)] \subseteq [\psi, \theta_1]$, $F^2 = F_3 \circ F_3$ is a contraction on $[v^*, m]$. Similarly, $F^2 = F_1 \circ F_1$ is a contraction on $[-m, -v^*]$. Therefore $F^4 = F_1^2 \circ F_3^2$ is a contraction on $[v^*, m]$ and therefore the period-4 orbit is unique and globally attracting. ■

3.2. Existence of period $2k$ and coexistence of periods $2k$ and $2(k + 1)$ for $k > 1$

We are now in a position to continue the mathematical induction process for k . Let α keep increasing past those values $\tilde{\alpha}_1 = 2.6694, \tilde{\alpha}_2 = 2.9131, \tilde{\alpha}_3 = 2.9664, \tilde{\alpha}_4 = 4, \tilde{\alpha}_5 = 5.2935$, given in the statements of Theorems 3.1–3.5. We obtain the following.

Lemma 3.5 (Key Lemma). *Let $\theta_n, n = 1, 2, \dots$, be defined as in (31). Then for each $n \in \mathbb{Z}^+$, there exists a unique strictly increasing sequence $\{\alpha_n | n = 1, 2, \dots, \alpha_n \geq 4\}$ such that $v^* = v^*(\alpha, \beta) \geq \theta_n = \theta_n(\alpha, \beta)$ if and only $\alpha \geq \alpha_n$.*

Proof. We use mathematical induction.

For $n = 1$, by Lemma 3.4(vi), we have $v^* \geq \theta_1$ if and only if $\alpha \geq \alpha_1 \equiv 4$.

Let it be true that $v^*(\alpha, \beta) \geq \theta_{n-1}(\alpha, \beta)$ if and only if $\alpha \geq \alpha_{n-1} > \alpha_{n-2} > \dots > \alpha_1 = 4$.

We make two claims:

- (i) For each $\alpha > 1, -\hat{v}(\alpha, \beta) < \theta_1(\alpha, \beta) < \theta_2, (\alpha, \beta) < \dots < \theta_k(\alpha, \beta) < \dots$; (54)
- (ii) For each $\alpha > 1$ and $c_j = c_j(\alpha)$, the solution of (37), $c_j(\alpha)$ is an increasing function of α such that $c_j(\alpha) \uparrow -1$ as $\alpha \uparrow \infty$, for any $j \in \mathbb{Z}^+$. (55)

Their verifications are straightforward and omitted.

Now let $\alpha \geq \alpha_{n-1}$. Then since $\theta_n > -\hat{v}$ by (i), by Lemmas 3.2 and 3.4(viii) we have $v^* \geq \theta_n$ if and only if $F_3(v^*) = v^* - 2x^* \geq F_3(\theta_n) = \theta_{n-1}$ and, thus,

$$\frac{v^* - 2x^*}{x^*} \geq \frac{\theta_{n-1}}{x^*},$$

$$\frac{\alpha - 1}{3} - 2 \geq - \left(\sum_{i=1}^{n-1} c_i + \frac{\alpha - 1}{3} \right), \quad \text{by (25), (38),}$$

$$\frac{2\alpha - 8}{3} \geq - \sum_{i=1}^{n-1} c_i(\alpha). \tag{56}$$

The RHS of (56) is a decreasing function of α by claim (ii) above, and

$$\lim_{\alpha \rightarrow \infty} \left[- \sum_{i=1}^{n-1} c_i(\alpha) \right] = n - 1,$$

while the LHS of (56) grows to $+\infty$ as $\alpha \rightarrow \infty$. Obviously, the inequality (56) will be satisfied if $\alpha \geq \alpha_n$, where $\alpha = \alpha_n$ makes (56) an equality. This α_n is unique satisfying $\alpha_n > \alpha_{n-1}$, as shown in Fig. 7. Therefore $v^* \geq \theta_n$ if and only if $\alpha \geq \alpha_n > \alpha_{n-1}$.

The proof is complete. ■

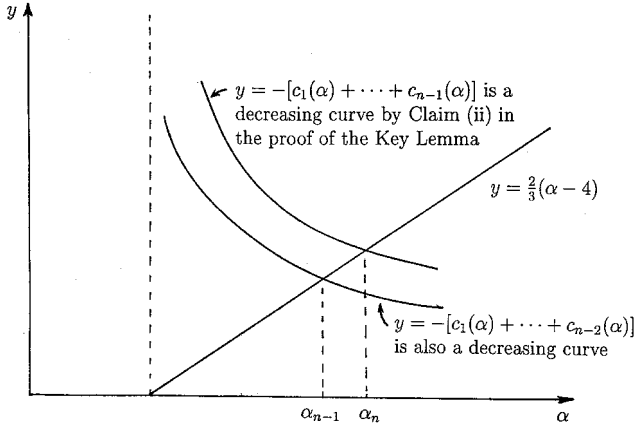


Fig. 7. The determination of α_n as the intersection of the line $y = (2/3)(\alpha - 4)$ and a decreasing curve $y = c_1(\alpha) + \dots + c_{n-1}(\alpha)$.

Since $-v^* < -\hat{v}$, from the strictly monotone increasing property of F_3 on $[-\hat{v}, \infty)$, (31)₂ and (54), we have

$$\theta_k < \zeta_k, \quad k \in \mathbb{Z}^+.$$

The possible relative positions between θ_k , ζ_k and m are:

$$m < \theta_k < \zeta_k, \quad \theta_k \leq m < \zeta_k \quad \text{and} \quad \theta_k < \zeta_k \leq m. \tag{57}$$

We discuss each of them sequentially in Theorems 3.6–3.8.

Theorem 3.6 (Existence of a Period-2k orbit). *Let $\alpha_{k-1} \leq \alpha < \alpha_k$ so that $\theta_{k-1} \leq v^* < \theta_k$, for some $k > 2$. If $m < \theta_k < \zeta_k$, then there exists a period-2k point $\xi \in [v^*, m]$.*

If, in addition, $F_3^{k-1}(v^) > \psi$ is satisfied, where ψ is the unique point in $(-v^*, -\hat{v})$ such that $F_3'(\psi) = -1$, then the period-2k orbit is unique and globally attracting.*

Proof. Since $\theta_{k-1} \leq v^* < m < \theta_k$, by the monotonicity of F_3 on $[-\hat{v}, \infty)$, we have $F_3^j(\theta_{k-1}) = \theta_{k-j-1} \leq F_3^j(v^*) < F_3^j(m) < F_3^j(\theta_k) = \theta_{k-j}$, for $j = 1, 2, \dots, k - 1$. Therefore

$$\begin{aligned} F_3^{k-1} : [v^*, m] &\xrightarrow{F_3} [F_3(v^*), F_3(m)] \xrightarrow{F_3} \dots \xrightarrow{F_3} [F_3^{k-1}(v^*), F_3^{k-1}(m)] \\ &\subseteq [F_3^{k-1}(\theta_{k-1}), F_3^{k-1}(\theta_k)] = [-v^*, \theta_1], \\ F_3^k([v^*, m]) &\subseteq [F_3(-v^*), F_3(\theta_1)] \subseteq [-m, -v^*], \quad \text{by Proposition 3.1,} \end{aligned} \tag{58}$$

Similarly, by symmetry, $F_1^k([-m, -v^*]) \subseteq [v^*, m]$. Therefore

$$F^{2k} = F_1^k \circ F_2^k : [v^*, m] \rightarrow [v^*, m].$$

By the Intermediate Value Theorem, $F_1^k \circ F_2^k$ has a fixed point $\xi \in [v^*, m]$, which is a period-2k point of F .

If $F_3^{(k-1)}(v^*) > \psi$, then using (58) we get

$$\begin{aligned} F_3^{k-1} : [v^*, m] &\xrightarrow{F_3} \dots \xrightarrow{F_3} [F_3^{k-1}(v^*), F_3^{k-1}(m)] \subseteq [\psi, F_3^{k-1}(\theta_k)] = [\psi, \theta_1], \\ F_3^k : [v^*, m] &\xrightarrow{F_3} \dots \xrightarrow{F_3} [\psi, \theta_1] \xrightarrow{F_3} [-m, -v^*], \quad \text{by Proposition 3.1,} \end{aligned} \tag{59}$$

where on each leg of the mapping chain (59), F_3 is contractive. By symmetry, the same can be said about

$$F_1^k : [-m, -v^*] \xrightarrow{F_1} \dots \xrightarrow{F_1} [-\theta_1, -\psi] \xrightarrow{F_1} [v^*, m].$$

Therefore $F^{2k} = F_1^k \circ F_3^k : [v^*, m] \rightarrow [v^*, m]$ is a contraction, with a unique fixed point $\xi \in [v^*, m]$ which is a periodic point of prime period $2k$ of F .

A little further discussion shows that every point on $[-m, m]$ will be eventually mapped into $[v^*, m]$, and so the period-2k orbit of ξ is globally attracting. We omit the details. ■

The second case in (57) is now covered in the following theorem, which indicate the presence of combination tones.

Theorem 3.7 (Existence of a Period 2k Attracting Orbit or Coexistence of Period-2k and $2(k + 1)$ Orbits). *Let $k > 2$, $\alpha_{k-1} \leq \alpha < \alpha_k$ so that $\theta_{k-1} \leq v^* < \theta_k$. If $\theta_k \leq m < \zeta_k$, then there exists a unique period-2k point $\xi_1 \in (\zeta_{k-1}, m]$ whose period-2k orbit has a domain of attraction containing $[\zeta_{k-1}, m]$.*

If in addition, $v^* + x^* > \theta_k$, then there also exists a period- $2(k + 1)$ point $\xi_2 \in [\theta_k, m] \setminus [\zeta_{k-1}, m]$.

Proof. Since $\theta_k \leq m < \zeta_k$, we have $v^* < \zeta_{k-1} < \theta_k \leq m < \zeta_k$, and so

$$F_3^k : [\zeta_{k-1}, m] \xrightarrow{F_3} [\zeta_{k-2}, F_3(m)] \xrightarrow{F_3} \cdots \xrightarrow{F_3} [\zeta_1, F_3^{k-2}(m)] \\ \xrightarrow{F_3} [-\hat{v}, F_3^{k-1}(m)] \xrightarrow{F_3} [-m, F_3^k(m)] \subseteq [-m, -\zeta_{k-1}],$$

because F_3 is contractive on each leg of the above chain. Similarly,

$$F_1^k : [-m, -\zeta_{k-1}] \xrightarrow{F_1} \cdots \xrightarrow{F_1} (\zeta_{k-1}, m].$$

Therefore by Proposition 3.1, $F^{2k} = F_1^k \circ F_3^k : [\zeta_{k-1}, m] \rightarrow [\zeta_{k-1}, m]$, and there exists a unique period- $2k$ point $\xi_1 \in (\zeta_{k-1}, m]$ whose orbit has a domain of attraction containing $[\zeta_{k-1}, m]$.

If in addition, $v^* + x^* > \theta_k$, then

$$F_3(-v^*) = -(v^* + x^*) < -\theta_k,$$

and so we have

$$F_3^{k+1} : [\theta_k, \zeta_k] \xrightarrow{F_3} [\theta_{k-1}, \zeta_{k-1}] \xrightarrow{F_3} \cdots \xrightarrow{F_3} [\theta_1, \zeta_1] \xrightarrow{F_3} [-v^*, -\hat{v}] \\ \xrightarrow{F_3} [-m, F(-v^*)] = [-m, -(v^* + x^*)] \subseteq [-\zeta_k, -\theta_k].$$

Similarly, $F_1^{k+1} : [-\zeta_k, -\theta_k] \rightarrow \cdots \rightarrow [F_1(v^*), m] \subseteq [\theta_k, \zeta_k]$. Therefore $F^{2(k+1)} = F_1^{k+1} \circ F_3^{k+1} : [\theta_k, \zeta_k] \rightarrow [\theta_k, \zeta_k]$ has a fixed point $\xi_2 \in [\theta_k, \zeta_k]$, which has prime period $2(k + 1)$. In view of the first half of the proof, we therefore have $\xi_2 \in [\theta_k, \zeta_k] \setminus [\zeta_{k-1}, m]$. But (m, ζ_k) is outside the global attractor $[-m, m]$. Hence we have $\xi_2 \in [\theta_k, m] \setminus [\zeta_{k-1}, m]$. ■

Finally, consider the third case in (57).

Theorem 3.8 (Coexistence of Period $2k$ and $2(k + 1)$ Attracting Orbits). *Let $\alpha_{k-1} \leq \alpha < \alpha_k$ so that $\theta_{k-1} \leq v^* < \theta_k$, where $k \in \mathbb{Z}^+$, $k > 1$. If $\theta_k < \zeta_k \leq m$, then there exists a unique period- $2k$ point $\xi_1 \in [v^*, \theta_k)$ whose period- $2k$ orbit is attracting on $[v^*, \theta_k]$, and there exists a unique period- $2(k + 1)$ point $\xi_2 \in (\zeta_k, m]$ whose period- $2(k + 1)$ orbit is attracting on $[\zeta_k, m]$.*

Proof. We have

$$F_3^k : [v^*, \theta_k] \xrightarrow{F_3} [F_3(v^*), \theta_{k-1}] \xrightarrow{F_3} [F_3^2(v^*), \theta_{k-2}] \rightarrow \cdots \xrightarrow{F_3} [F_3^{k-1}(v^*), \theta_1] \xrightarrow{F_3} (-\theta_k, -v^*), \quad (60)$$

where the last leg of the chain in (60) holds because

$$-\hat{v} = F_3^k(\zeta_k) < F_3^{k-1}(v^*) < F_3^{k-1}(\theta_k) = \theta_1, \quad \text{and} \quad 0 < F_3^j(v) < 1 \quad \text{on} \quad [F_3^j(v^*), \theta_{k-j}], \quad j = 0, \dots, k - 1. \quad (61)$$

Similarly,

$$F_1^k : [-\theta_k, -v^*] \xrightarrow{F_1} [-\theta_{k-1}, F_1(-v^*)] \xrightarrow{F_1} [-\theta_{k-2}, F_1^2(-v^*)] \rightarrow \cdots \xrightarrow{F_1} [v^*, \theta_k]. \quad (62)$$

By (60)–(62), we have

$$F^{2k} = F_1^k \circ F_3^k : [v^*, \theta_k] \rightarrow [v^*, \theta_k]$$

is a contraction with a unique fixed point $\xi_1 \in [v^*, \theta_k)$. The point ξ_1 has period $2k$, the domain of attraction of whose orbit contains $[v^*, \theta_k]$.

Next, let $\zeta_k < m$. Then

$$F_3^{k+1} : [\zeta_k, m] \xrightarrow{F_3} [\zeta_{k-1}, F_3(m)] \xrightarrow{F_3} \dots \xrightarrow{F_3} [\zeta_1, F_3^{k-1}(m)] \\ \xrightarrow{F_3} [-\hat{v}, F_3^k(m)] \xrightarrow{F_3} [-m, -\zeta_k] \subseteq [-m, -v^*]$$

because $0 < F_3'(v) < 1$ holds on each leg of the mapping chain. Similarly,

$$F_1^{k+1} : [-m, -\zeta_k] \xrightarrow{F_1} [F_1(-m), -\zeta_{k-1}] \longrightarrow \dots \xrightarrow{F_1} (\zeta_k, m] \subseteq (v^*, m].$$

Therefore $F^{2k+2} = F_1^{k+1} \circ F_3^{k+1} : [\zeta_k, m] \longrightarrow [\zeta_k, m]$ is a contraction with a unique fixed point $\xi_2 \in (\zeta_k, m]$. This point ξ_2 has period $2(k+1)$, the domain of attraction of whose orbit contains $[\zeta_k, m]$.

If $\zeta_k = m$, from the argument in the above paragraph, by letting $\zeta_k \rightarrow m$ we easily see that ζ_k itself has prime period $2(k+1)$. The period- $2(k+1)$ orbit of ζ_k has a domain of attraction containing $[\zeta_k - \varepsilon, \zeta_k + \varepsilon]$ for some small $\varepsilon > 0$ because $0 = F_3'(-\hat{v}) = F_3'(F_3^k(\zeta_k))$. ■

Remark 3.2.

- (1) In Theorem 3.6, if the additional assumption $F_3^{k-1}(v^*) > \psi$ is violated, then we suspect that there may exist both stable and unstable orbits of periods other than $2k$, such as what Theorem 3.2 has shown. We conjecture that if they do exist, they are of periods $2(k+1)$.
- (2) In Theorems 3.7 and 3.8, we have established the existence and some partial uniqueness and stability results of period- $2k$ and period- $2(k+1)$ orbits. Through numerical simulations, we have found that these orbits appear to be the *only stable orbits* in existence. See Examples 3.1–3.3. We suspect that these periodic orbits captured by us constitute the *only stable periodic orbits* under the assumptions of Theorems 3.7 and 3.8.

Example 3.1. Let $\alpha = 45, \beta = 1$. Using (25), (27) Lemmas 3.2 and 3.3, we have computed and obtained the following values:

$$v^* = 56.1691, \quad m = 60.0420, \quad \theta_{17} = 52.7489, \\ \zeta_{17} = 52.8225, \quad \theta_{18} = 60.4728, \quad \zeta_{18} = 60.5475.$$

We get the following relative positioning of these points:

$$\theta_{17} < \zeta_{17} < v^* < m < \theta_{18} < \zeta_{18}. \quad (63)$$

Therefore Theorem 3.6 applies with $k = 18$. There exists a period-36 orbit. This orbit is clearly displayed in Fig. 8. It is the only stable periodic orbit which has emerged after thorough numerical simulations.

Example 3.2. Let $\alpha = 45.15, \beta = 1$. Then we obtain

$$v^* = 56.4565, \quad m = 60.3359, \quad x^* = 3.8362, \\ \theta_{17} = 52.5666, \quad \zeta_{17} = 52.6400, \\ \theta_{18} = 60.2965, \quad \zeta_{18} = 60.3710.$$

These values satisfy

$$\theta_{17} < \zeta_{17} < v^* < \theta_{18} < m < \zeta_{18}. \quad (64)$$

Therefore the first part of Theorem 3.7 applies with $k = 18$. There exists a stable period $2k = 36$ orbit.

The second part of Theorem 3.7 does not apply because

$$v^* + x^* = 60.2927 < \theta_{18} = 60.2965.$$

From numerical simulations, we nevertheless have found that a second stable period-38 ($2(k+1) = 2(18+1) = 38$) orbit exists.

This example seems to suggest that the condition of $\theta_k < \zeta_k < v^* < \theta_{k+1} < m < \zeta_k$ alone is sufficient to guarantee the coexistence of the stable period- $2k$ and period- $2(k+1)$ orbits, without requiring $v^* + x^* > \theta_{k+1}$. But so far we have not been able to prove it.

The coexistence of stable period-36 and 38 orbits can be seen in Fig. 9.

When $\alpha = 45.16$, we have

$$v^* = 56.4757, \quad m = 60.3555, \quad x^* = 3.8367, \\ v^* + x^* = 60.3124, \quad \theta_{17} = 52.5544, \\ \zeta_{17} = 52.6278, \quad \theta_{18} = 60.2847, \quad \zeta_{18} = 60.3592,$$

hence

$$\theta_{17} < \zeta_{17} < v^* < \theta_{18} < v^* + x^* < m < \zeta_{18},$$

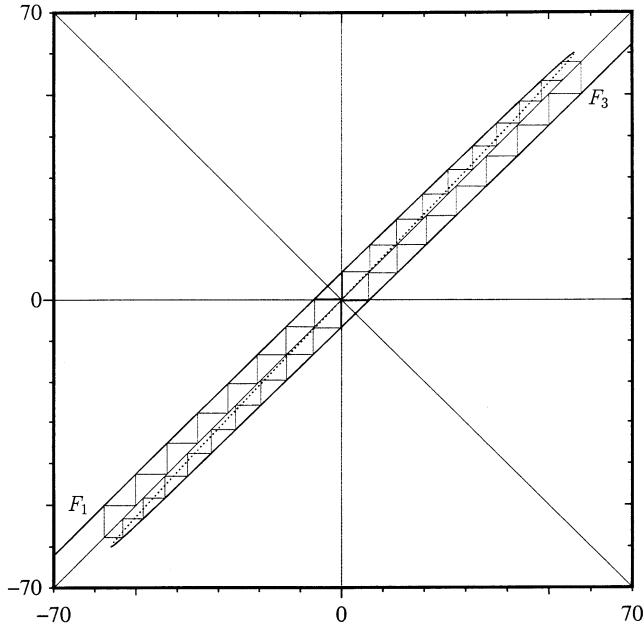


Fig. 8. A stable period-36 orbit for the hysteresis map F in Example 3.1, where $\alpha = 45$, $\beta = 1$ and $k = 18$ (in Theorem 3.6). The dotted line represents the F_2 branch.

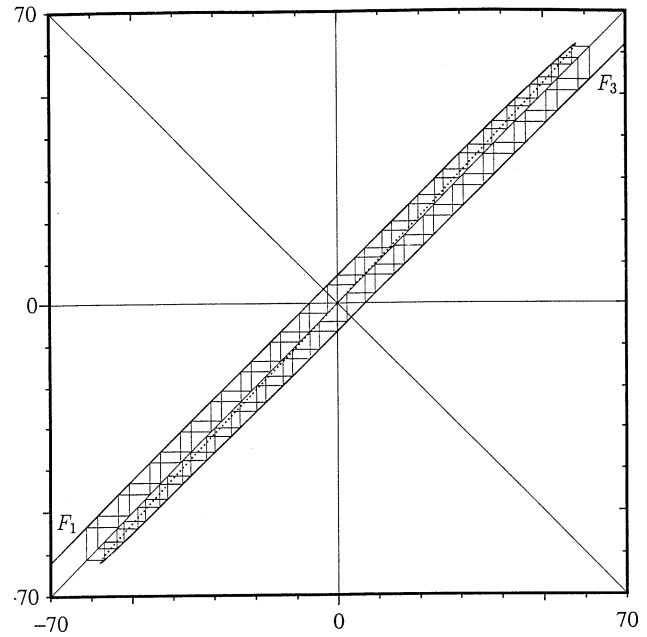


Fig. 10. Coexistence of stable period-36 and period-38 orbits for the hysteresis map F in Example 3.3, where $\alpha = 46$ and $\beta = 1$. Theorem 3.8 applies for $k = 18$. The dotted line represents the F_2 branch.

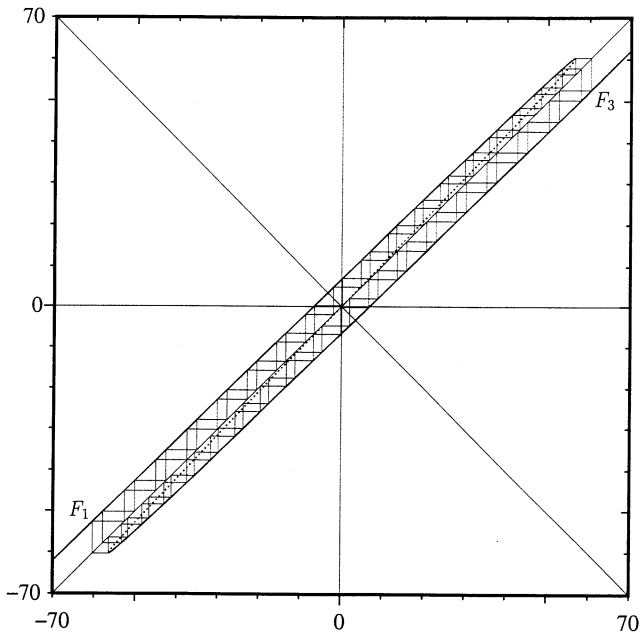


Fig. 9. Coexistence of stable period-36 and period-38 orbits for the hysteresis map F in Example 3.2, where $\alpha = 45.15$, $\beta = 1$. The dotted line represents the F_2 branch. Note that the assumption of the second half of Theorem 3.7 is violated.

and all the conditions in Theorem 3.7 are fulfilled for $k = 18$. By Theorem 3.7, there is of course the coexistence of stable period-36 and 38 orbits (which look almost identical to those in Fig. 9 and therefore are omitted).

If $\alpha = 45.14$, then (63) still holds but (64) is violated. Theorem 3.6 now applies. We have found only a stable period-36 orbit through simulations.

Example 3.3. Let $\alpha = 46$, $\beta = 1$. Then

$$\begin{aligned} v^* &= 58.0948, & m &= 62.0105, & \theta_{17} &= 51.5214, \\ \zeta_{17} &= 51.5939, & \theta_{18} &= 59.2850, & \zeta_{18} &= 59.3585, \\ \theta_{19} &= 67.1623, & \zeta_{19} &= 67.2369. \end{aligned}$$

We have

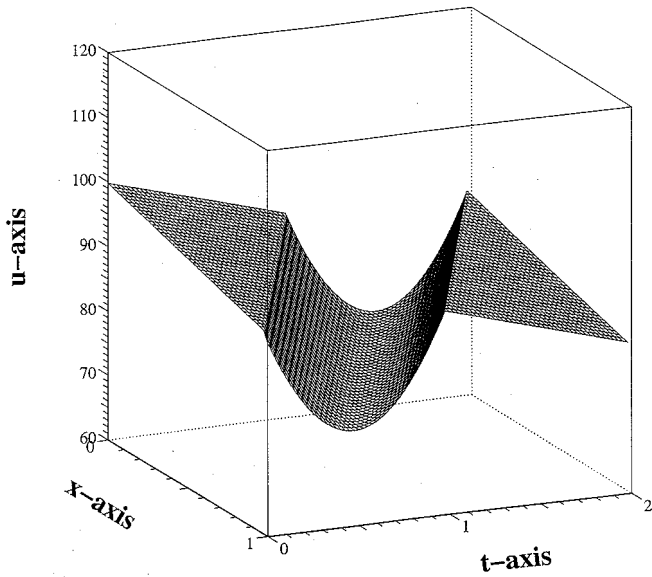
$$\theta_{17} < \zeta_{17} < v^* < \theta_{18} < \zeta_{18} < m < \theta_{19} < \zeta_{19}.$$

Therefore Theorem 3.8 is applicable with $k = 18$. There is the coexistence of a stable period-36 orbit with another stable period-38 orbit. See Fig. 10.

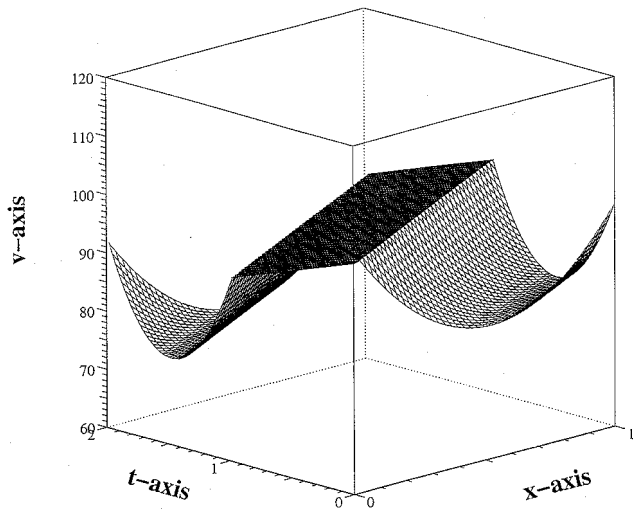
Example 3.4. Let $\alpha = 45$, $\beta = 1$. Let the initial conditions for u_0 and v_0 in (23)₄ be

$$\begin{aligned} u_0(0) &= v_0(0) = 100, \\ u_0(1) &= F_3(v_0(1)), & v_0(1) &\equiv 100, \\ u_0(x) &= u_0(0) + x[u_0(1) - u_0(0)], & x &\in (0, 1), \\ v_0(x) &= u_0(x)^2 + b_{\alpha,\beta}u_0(x) + c_{\alpha,\beta}, & x &\in (0, 1), \end{aligned} \tag{65}$$

where $b_{\alpha,\beta} = -191.74$ and $c_{\alpha,\beta} = 9274.07$ are two constants chosen to satisfy $v_0(0) = v_0(1) = 100$.



(a) u



(b) v

Fig. 11. The solution profiles for $u(x, t)$ and $v(x, t)$, for $t \in [0, 2]$, in Example 3.4.

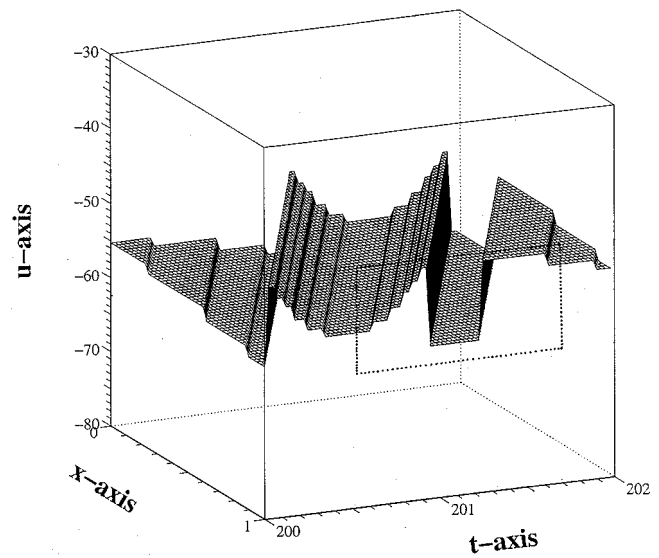
We solve the solution $(u(x, t), v(x, t))$ of the system of (9). Note that the initial conditions in (65) satisfy the compatibility conditions

$$v_0(0) = u_0(0),$$

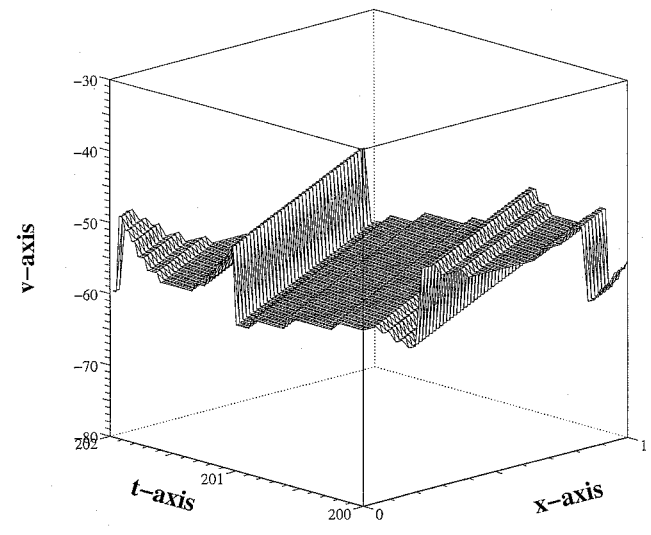
$$\beta[u_0(1) - v_0(1)]^3 + (1 - \alpha)[u_0(1) - v_0(1)] + 2v_0(1) = 0.$$

Also, u_0 and v_0 are continuous on $[0, 1]$.

The solution profiles of $u(x, t), v(x, t)$ for $t \in [0, 2]$ are displayed in Fig. 11. They are again displayed for $t \in [200, 202]$ in Fig. 12. The reader



(a) u



(b) v

Fig. 12. The solution profiles for $u(x, t)$ and $v(x, t)$, for $t \in [200, 202]$ in Example 3.4. A staircase-platform shape has emerged. Each platform value corresponds to one of the u values in the period-36 orbit shown in Fig. 8. A small window in (a) is zoomed in and displayed in Fig. 14(a).

may find that solutions u and v have evolved into a staircase-platform shape. Each platform value corresponds to one of the u values in the period-36 orbit shown in Fig. 8.

Example 3.5. We choose $\alpha = 46, \beta = 1$. Everything else remains the same as in Example 3.4 (Note: now $b_{\alpha,\beta} = -191.69$ and $c_{\alpha,\beta} = 9268.94$).

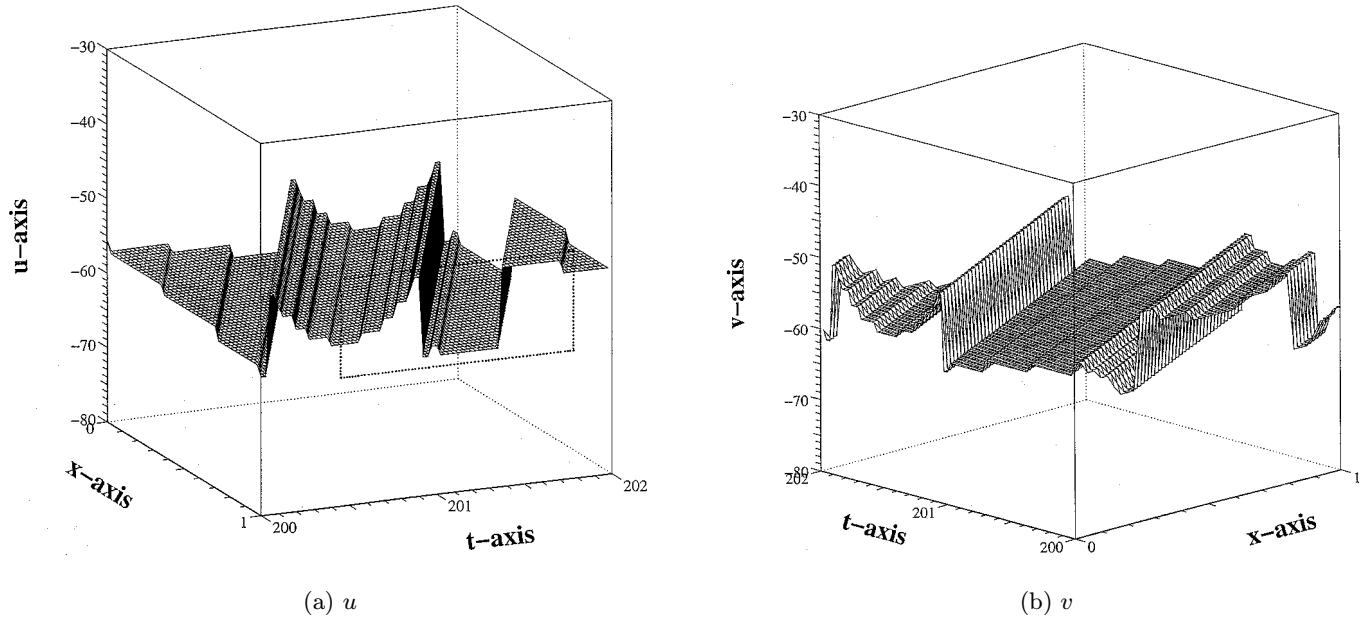


Fig. 13. The solution profiles for $u(x, t)$ and $v(x, t)$, for $t \in [200, 202]$ in Example 3.5, again with a staircase-platform shape. Each platform value corresponds to one of the u values in the period-36 or period-38 orbits shown in Fig. 10. A small window in (a) is zoomed in and displayed in Fig. 14(b) for comparison.

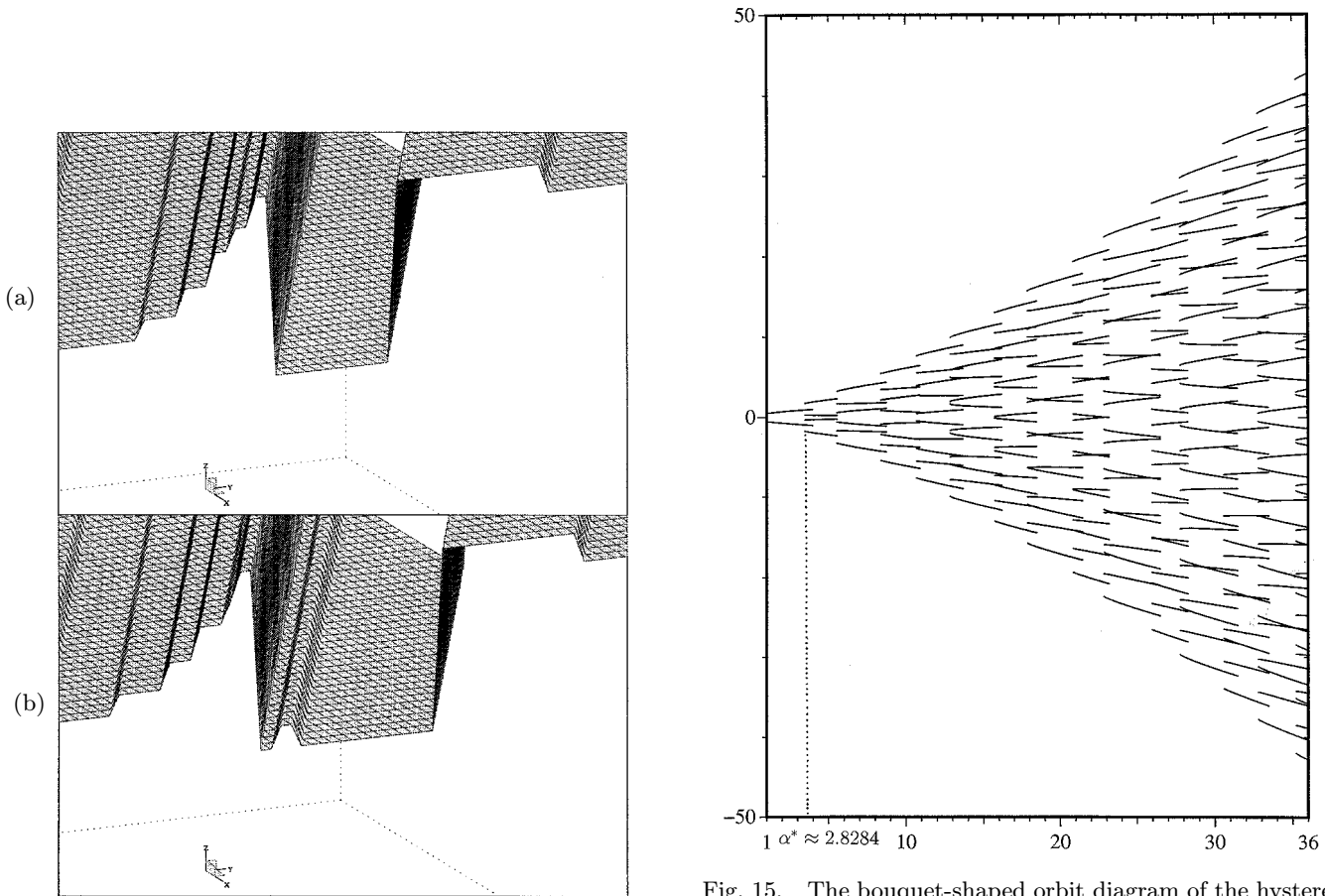


Fig. 14. Magnifications of the windows in Figs. 12(a) and 13(a) to show the difference between these profiles.

Fig. 15. The bouquet-shaped orbit diagram of the hysteresis map $F = F_{\alpha, \beta}$ in Example 3.6. We hold $\beta = 1$ fixed and let $\alpha \in [1, 36]$. Note that α^* is the first bifurcation point cited in Remark 3.1.

Now the hysteresis map F (in Example 3.3) has the coexistence of stable period-36 and period-38 orbits. The solution profiles of u and v for $t \in [200, 202]$ are illustrated in Fig. 13. To show the difference between Figs. 12 and 13, we have zoomed in on portions of Figs. 12 and 13 and made the comparison in Fig. 14.

Example 3.6. To conclude this section, we show the orbit diagram of the hysteresis map $F = F_{\alpha,\beta}$, where $\beta = 1$ is fixed, but $\alpha \in [1, 36]$. See Fig. 15. Note that α^* is the first bifurcation point cited in Remark 3.1.

4. Chaotic Vibrations Due to Natural Hysteresis and Energy Injection

We now consider the system (23), but with the left end boundary condition changed to (13). The overall system becomes

$$\left\{ \begin{array}{l} \text{PDE (6);} \\ \text{left end boundary condition } v = G(u) \equiv \frac{1 + \eta}{1 - \eta}u, \\ \quad \text{at } x = 0, \quad \text{for } t > 0; \\ \text{right end boundary condition } u = F(v), \\ \quad \text{at } x = 1, \quad \text{for } t > 0, \\ \quad \text{where } F \text{ is defined through (8);} \\ \text{initial conditions } u(x, 0) = \frac{1}{2}[w'_0(x) + w_1(x)], \\ \quad v(x, 0) = \frac{1}{2}[w'_0(x) - w_1(x)], \quad x \in (0, 1), \\ \text{cf. (4), (5).} \end{array} \right. \tag{66}$$

As discussed in Example 2.3, the solution can be determined by the multivalued, composite hysteresis curves $G \circ F$ and $F \circ G$, whose hysteresis iterates are already defined by Definition 2.1.

We may use Figs. 3 and 4 as a visual aid. Let v^* , \hat{v} , and m be defined as in (24)–(27). The treatments for $G \circ F$ and $F \circ G$ are essentially similar, so we will only treat $G \circ F$ here. Let us assume that for $0 < \eta < 1, 1 < \alpha < \infty, \beta > 0$,

$$\tilde{m} = \frac{1 + \eta}{1 - \eta}m \leq \frac{1 + \eta}{2\eta} \sqrt{\frac{1 + \alpha\eta}{\beta\eta}} \tag{67}$$

$$\left(m = \frac{1 + \alpha}{3} \sqrt{\frac{1 + \alpha}{3\beta}} \right)$$

is satisfied, cf. Part II [Chen *et al.*, 1998b, (40)]. Consequently, hysteresis iterates $(v_k, u_k), u_k =$

$\tilde{H}(v_k), \tilde{H} \equiv G \circ F$, stay within a bounded trapping region $[-\tilde{m}, \tilde{m}] \times [-\tilde{m}, \tilde{m}]$, for $v_k \in [-\tilde{m}, \tilde{m}]$.

Now, cf. (31) and define

$$\begin{aligned} \tilde{\theta}_0 &= \theta_0, \quad \tilde{\zeta}_0 = \zeta_0, \quad \tilde{v}^* = v^*, \\ \tilde{F}_i &= G \circ F_i, \quad i = 1, 2, 3, \\ \tilde{F}_3(\tilde{\theta}_{j+1}) &= \tilde{\theta}_j, \quad \tilde{F}_3(\tilde{\zeta}_{j+1}) = \tilde{\zeta}_j, \quad j = 0, 1, 2, \dots \end{aligned} \tag{68}$$

Since G is just the multiplication by $(1 + \eta)/(1 - \eta)$, Lemmas 3.1–3.4 in Sec. 3 are essentially applicable to $\tilde{F}_i, i = 1, 2, 3$, after a straightforward adaptation. We easily observe that we have the monotonicity

$$\tilde{\theta}_0 < \tilde{\zeta}_0 < \tilde{\theta}_1 < \tilde{\zeta}_1 < \dots < \tilde{\theta}_j < \tilde{\zeta}_j < \dots$$

Theorem 4.1 (Sufficient Condition for Chaos for the One-Dimensional Wave Equation with Energy Injecting and van der Pol Boundary Conditions). *Let $0 < \eta < 1, \alpha > 1, \beta > 0$, such that (67) holds. If for some $j \geq 1$, we have $\tilde{\theta}_{j-1} < \tilde{v}^*$; $\tilde{\theta}_j, \tilde{\theta}_{j+1}, \tilde{\theta}_{j+2} \in [\tilde{v}^*, \tilde{m}]$, then the hysteresis map $u = \tilde{H}(v), \tilde{H} = G \circ F$, is chaotic on the interval $[-\tilde{m}, \tilde{m}]$.*

Proof. We can ignore the “maiden voyage” part of the hysteresis iteration $u_k = \tilde{H}^k(u_0)$ as it only represents transient response. Thus now the hysteresis iteration is done only by iterations of \tilde{F}_1 and \tilde{F}_3 . We construct the following shift sequence:

$$\begin{aligned} I_0 &= [\tilde{\theta}_{j+1}, \tilde{\theta}_{j+2}], I_1 = [\tilde{\theta}_j, \tilde{\theta}_{j+1}], \dots, I_j \\ &= [\tilde{\theta}_1, \tilde{\theta}_2], I_{j+1} = [\tilde{\theta}_0, \tilde{\theta}_1]. \end{aligned}$$

Then $\tilde{F}_3(I_{j+1}) \subseteq [-\tilde{m}, -\tilde{v}^*]$. Further, let

$$\begin{aligned} \tilde{I}_{j+2} &= [-\tilde{\theta}_{j+1}, -\tilde{\theta}_j], \tilde{I}_{j+3} = [-\tilde{\theta}_j, -\tilde{\theta}_{j-1}], \dots, \tilde{I}_{2j+1} \\ &= [-\tilde{\theta}_2, -\tilde{\theta}_1], \tilde{I}_{2j+2} = [-\tilde{\theta}_1, -\tilde{\theta}_0]. \end{aligned}$$

Then

$$\tilde{F}_1(\tilde{I}_{2j+2}) = [\tilde{v}^*, \tilde{m}] \supseteq I_0 \cup I_1,$$

so we have the following shift sequence

$$\begin{aligned} I_0 &\xrightarrow{\tilde{F}_3} I_1 \xrightarrow{\tilde{F}_3} I_2 \longrightarrow \dots \xrightarrow{\tilde{F}_3} I_j \\ &\xrightarrow{\tilde{F}_3} I_{j+1} \xrightarrow{\tilde{F}_3} I_{j+2} \xrightarrow{\tilde{F}_1} I_{j+3} \longrightarrow \dots \\ &\xrightarrow{\tilde{F}_1} I_{2j+2} \xrightarrow{\tilde{F}_1} I_0 \cup I_1. \end{aligned} \tag{69}$$

Note that in the above, $\tilde{H}^{i+j+1}(u_0) = \tilde{F}_1^i \circ \tilde{F}_3^{j+1}(u_0)$ for any $i = 0, 1, \dots, j + 2$ by (an adapted version of) Proposition 3.1.

From the shift sequence (69), one can either use the rotation number as in [Keener, 1980] or Part I [Chen *et al.*, 1998a, Appendix A] or do symbolic dynamics as in [Devaney, 1989] [with a slight modification of the intervals in the sequence (69)] to show that \tilde{H} is chaotic. ■

Example 4.1. Theorem 4.1 offers a concrete way to verify the occurrence of chaos. Let us choose $\eta = 1/2, \alpha = 2, \beta = 1$. Then applying (a slightly modified version of) Lemmas 3.1–3.4, we have computed the following values:

$$\begin{aligned} \tilde{m} &= 3, \quad \frac{1 + \eta}{2\eta} \sqrt{\frac{1 + \alpha\eta}{\beta\eta}} = 3, \quad \text{so (67) holds,} \\ \tilde{v}^* &= 0.1925, \quad \tilde{\theta}_0 = -0.1925, \quad \tilde{\theta}_1 = 1.6461, \\ \tilde{\theta}_2 &= 2.4408, \quad \tilde{\theta}_3 = 2.7710, \quad \tilde{\theta}_4 = 2.9065, \\ &\dots, \quad \lim_{j \rightarrow \infty} \tilde{\theta}_j = 3; \quad \text{cf. Fig. 3.} \end{aligned}$$

Therefore, for $j = 1$, we have $\tilde{\theta}_{j-1} = \tilde{\theta}_0 = -\tilde{v}^* < \tilde{v}^*$, and

$$\tilde{v}^* < \tilde{\theta}_1 < \tilde{\theta}_2 < \tilde{\theta}_3 < \dots < \tilde{\theta}_n < \dots \rightarrow 3 = \tilde{m}, \tag{70}$$

i.e.

$$\tilde{\theta}_1, \tilde{\theta}_2, \dots, \tilde{\theta}_n, \dots \in [\tilde{v}^*, m]$$

for any positive integer n .

Therefore very strong chaos occurs.

Let us choose initial conditions $u_0(x)$ and $v_0(x)$ to be, respectively, linear and quadratic functions in the following way:

$$\begin{aligned} u_0(x) &= u_0(0) + x[u_0(1) - u_0(0)], \\ v_0(x) &= u_0(x)^2 + bu_0(x) + c, \end{aligned} \tag{71}$$

$u_0(0) = 0.5, v_0(0) = 1.5, v_0(1) = 1.5, u_0(1) = F(v_0(1))$. The unspecified constants b and c can then be determined as follows:

$$v_0(0) = u_0(0)^2 + bu_0(0) + c, \quad v_0(1) = u_0(1)^2 + bu_0(1) + c,$$

$$b = \frac{v_0(1) - v_0(0)}{u_0(1) - u_0(0)} - [u_0(0) + u_0(1)]; \quad (b = -0.32830)$$

$$v_0(0)u_0(1) - v_0(1)u_0(0) = u_0(0)^2u_0(1) - u_0(1)^2u_0(0) + c[u_0(1) - u_0(0)],$$

$$c = \frac{v_0(0)u_0(1) - v_0(1)u_0(0)}{u_0(1) - u_0(0)} + u_0(0)u_0(1); \quad (c = 1.41415).$$

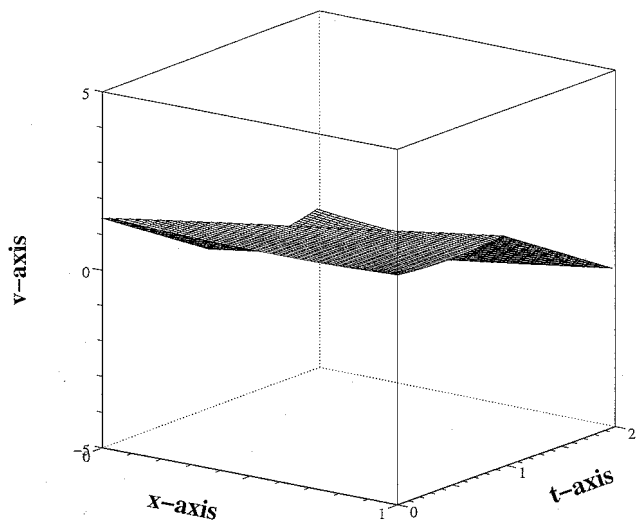
It is easy to check that, with the above choices, (C^0) compatibility conditions at the boundary points $x = 0, x = 1$, are satisfied by the initial data. We then compute $u(x, t), v(x, t)$ according to (15) and (16). The profiles for u and v , for $t \in [0, 2]$ and $t \in [200, 202]$, are displayed in Figs. 16 and 17. The reader may find strong chaotic vibrations in the spatio-temporal profiles in Fig. 17, as well as in the snapshots in Fig. 18.

Remark 4.1

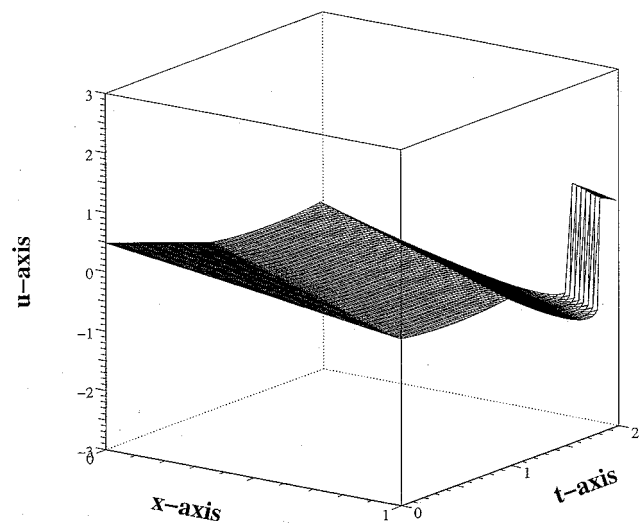
- (i) If the condition (67) is violated, one can still construct a Cantor-like invariant set $C \subseteq [-\tilde{m}, \tilde{m}]$ where \tilde{H} is chaotic, similar to Part II [Chen *et al.*, 1998b, Sec. 5]

- (ii) Example 4.1, particularly (70) shows that there exists an $\tilde{\eta} : 0 < \tilde{\eta} < 0.5$ such that Theorem 4.1 holds for all $\eta \in (\tilde{\eta}, 0.5), \alpha = 2, \beta = 1$.

Remark 4.2. When $\eta = 0$ in (66), the system (66) reduces to system (23) in Sec. 3, and $\tilde{\theta}_i$ in (68) reduces to the θ_i in Lemma 3.2. One can easily show that the condition $\theta_j, \theta_{j+1}, \theta_{j+2} \in [v^*, m]$ will never be satisfied. Thus Theorem 4.1 is definitely not applicable when $\eta = 0$. This offers some additional credence that the hysteresis map in Sec. 3, without additional energy injection from the left end $x = 1$, is not chaotic.

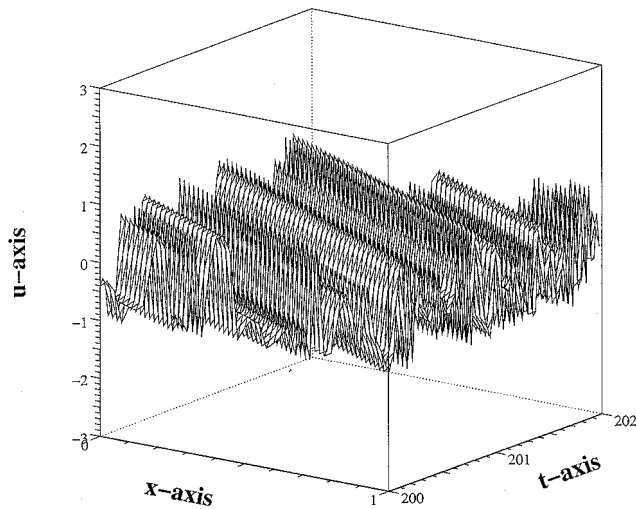


(a) u

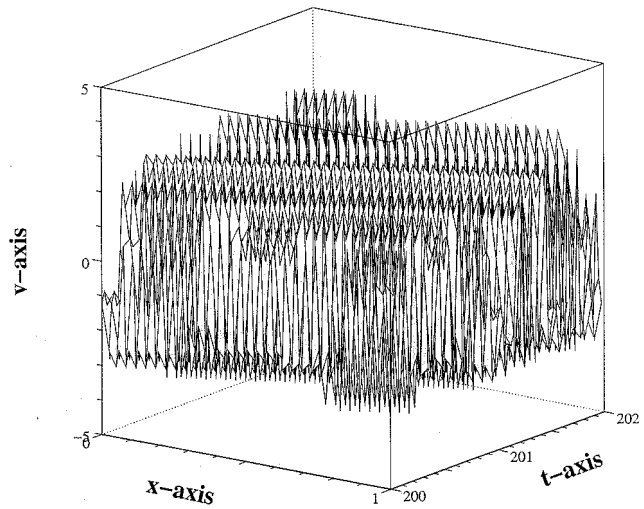


(b) v

Fig. 16. The solution $u(x, t)$ and $v(x, t)$, for $t \in [0, 2]$ in Example 4.1, where $\alpha = 2$, $\beta = 1$, $\eta = 1/2$.

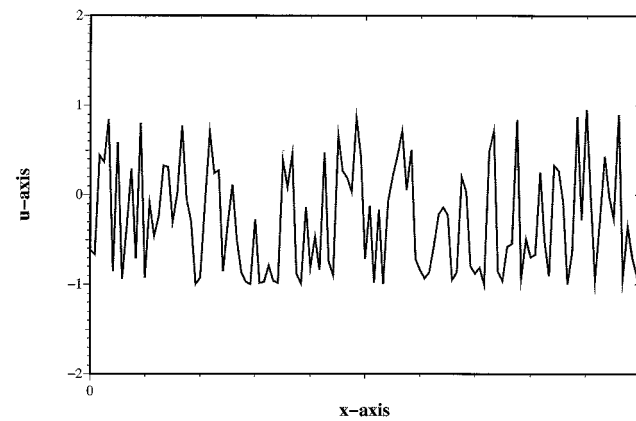


(a) u

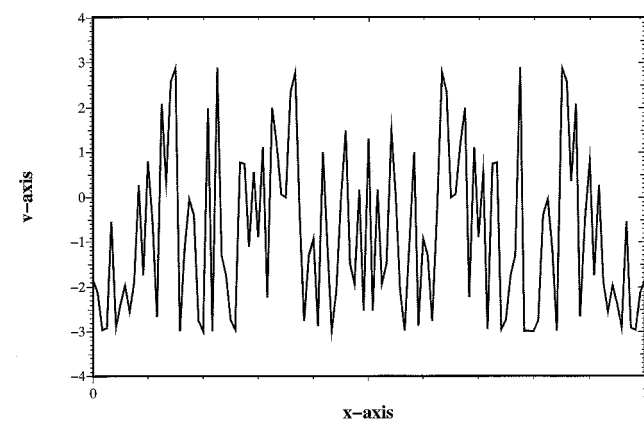


(b) v

Fig. 17. The solution $u(x, t)$ and $v(x, t)$, for $t \in [200, 202]$ in Example 4.1. Observe the spatiotemporal chaotic profiles.



(a)



(b)

Fig. 18. Snapshots of the solution (a) $u(x, t)$ and (b) $v(x, t)$, $0 \leq x \leq 1$, for $t = 202$, for Example 4.1, where $\alpha = 2$, $\beta = 1$, $\eta = 1/2$.

Acknowledgments

G. Chen and J. Zhou were partially supported by NSF Grants DMS 9404380 and 9610076, Texas ARP Grant 010366-046, and Texas A&M University IRI 96-36. S. B. Hsu was partially supported by a research grant from the National Council of Science of Republic of China.

References

- Chen, G., Hsu, S. B. & Zhou, J. [1998a] "Chaotic vibrations of the one-dimensional wave equation due to a self-excitation boundary condition, Part I: Controlled hysteresis," *Trans. Amer. Math. Soc.*, to appear.
- Chen, G., Hsu, S. B. & Zhou, J. [1998b] "Chaotic vibrations of the one-dimensional wave equation due to a self-excitation boundary condition. II. Energy injection, periodic doubling and homoclinic orbits," *Int. J. Bifurcation and Chaos* **8**(3), 423–445.
- Chern, C. J. [1995] "On an iterative process describing natural hysteresis," Masters Thesis, Institute of Applied Mathematics, Tsing Hua University, Hsinchu, Taiwan, R.O.C., May 1995.
- Devaney, R. L. [1989] *An Introduction to Chaotic Dynamical Systems* (Addison-Wesley, New York).
- Keener, J. P. [1980] "Chaotic behavior in piecewise continuous difference equations," *Trans. Amer. Math. Soc.* **261**, 589–604.
- Parker, S. P. *et al.* [1982] *McGraw-Hill Encyclopedia of Physics* (McGraw-Hill, New York).
- Stoker, J. J. [1950] *Nonlinear Vibrations* (Wiley-Interscience, New York).
- Visintin, A. [1986] "A model for hysteresis in distributed systems," *Math. Zeit.* **193**, 247–264.